



Contents lists available at ScienceDirect

Science of the Total Environment

journal homepage: [www.elsevier.com/locate/scitotenv](http://www.elsevier.com/locate/scitotenv)

## Environmental baseline monitoring for shale gas development in the UK: Identification and geochemical characterisation of local source emissions of methane to atmosphere

David Lowry<sup>a,\*</sup>, Rebecca E. Fisher<sup>a</sup>, James L. France<sup>a,b</sup>, Max Coleman<sup>a</sup>, Mathias Lanoisellé<sup>a</sup>, Giulia Zazzeri<sup>a,1</sup>, Euan G. Nisbet<sup>a</sup>, Jacob T. Shaw<sup>c</sup>, Grant Allen<sup>c</sup>, Joseph Pitt<sup>c</sup>, Robert S. Ward<sup>d</sup>

<sup>a</sup> Department of Earth Sciences, Royal Holloway, University of London, Egham TW20 0EX, UK

<sup>b</sup> British Antarctic Survey, High Cross, Madingley Rd, Cambridge CB3 0ET, UK

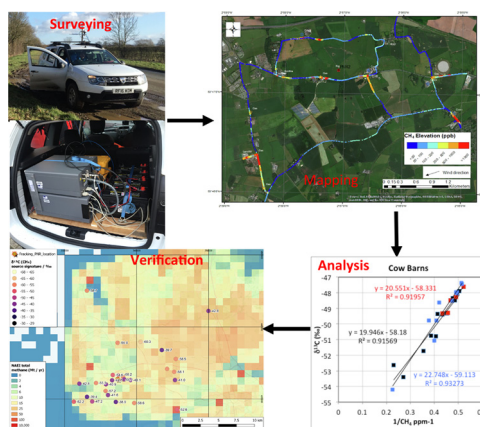
<sup>c</sup> School of Earth and Environmental Science, University of Manchester, M13 9PL, UK

<sup>d</sup> British Geological Survey, Environmental Science Centre, Keyworth, Nottingham NG12 5GG, UK

### HIGHLIGHTS

- Seasonal surveys to identify CH<sub>4</sub> sources near planned unconventional gas extraction.
- Mobile measurement of CH<sub>4</sub> and C<sub>2</sub>H<sub>6</sub> with subsequent GIS mapping.
- Sample collection for carbon isotope analysis of CH<sub>4</sub>.
- Characterization of methane sources into fossil fuel, waste and farming categories.
- Potential fugitive emissions from unconventional gas could be identified.

### GRAPHICAL ABSTRACT



### ARTICLE INFO

#### Article history:

Received 18 July 2019

Received in revised form 19 September 2019

Accepted 20 September 2019

Available online xxxxx

#### Keywords:

Mobile measurement

Baseline surveys

Methane

Carbon isotopes

Ethane

### ABSTRACT

Baseline mobile surveys of methane sources using vehicle-mounted instruments have been performed in the Fylde and Ryedale regions of Northern England over the 2016–19 period around proposed unconventional (shale) gas extraction sites. The aim was to identify and characterise methane sources ahead of hydraulically fractured shale gas extraction in the area around drilling sites. This allows a potential additional source of emissions to atmosphere to be readily distinguished from adjacent sources, should gas production take place.

The surveys have used ethane:methane (C<sub>2</sub>:C<sub>1</sub>) ratios to separate combustion, thermogenic gas and biogenic sources. Sample collection of source plumes followed by high precision δ<sup>13</sup>C analysis of methane, to separate and isotopically characterise sources, adds additional biogenic source distinction between active and closed landfills, and ruminant eructations from manure.

The surveys show that both drill sites and adjacent fixed monitoring sites have cow barns and gas network pipeline leaks as sources of methane within a 1 km range. These two sources are readily separated by isotopes (δ<sup>13</sup>C of −67 to −58‰ for barns, compared to −43 to −39‰ for gas leaks), and ethane:methane ratios (<0.001 for barns, compared to >0.05 for gas leaks). Under a well-mixed daytime

\* Corresponding author.

E-mail address: [d.lowry@rhul.ac.uk](mailto:d.lowry@rhul.ac.uk) (D. Lowry).

<sup>1</sup> Now at Department of Physics, Imperial College London, Kensington, London SW7 2AZ, UK.

<https://doi.org/10.1016/j.scitotenv.2019.134600>

0048-9697/© 2019 The Author(s). Published by Elsevier B.V.

This is an open access article under the CC BY-NC-ND license (<http://creativecommons.org/licenses/by-nc-nd/4.0/>).

Please cite this article as: D. Lowry, R. E. Fisher, J. L. France et al., Environmental baseline monitoring for shale gas development in the UK: Identification and geochemical characterisation of local source emissions of methane to atmosphere, Science of the Total Environment, <https://doi.org/10.1016/j.scitotenv.2019.134600>

atmospheric boundary layer these sources are generally detectable as above baseline elevations up to 100 m downwind for gas leaks and up to 500 m downwind for populated cow barns. It is considered that careful analysis of these proxies for unconventional production gas, if and when available, will allow any fugitive emissions from operations to be distinguished from surrounding sources.

© 2019 The Author(s). Published by Elsevier B.V. This is an open access article under the CC BY-NC-ND license (<http://creativecommons.org/licenses/by-nc-nd/4.0/>).

## 1. Introduction

Unconventional gas extraction and hydraulic fracturing has a long history in the UK, but the search for shale gas, and opposition to it, has gathered momentum since 2015 and the 14th round of Petroleum Exploration and Development Licenses (Priestley, 2018). The potential for greenhouse gas emissions from the development of shale gas extraction and use in relation to UK shale gas development had been identified by McKay and Stone (2013), and requirements for baseline monitoring prior to drilling and extraction were put in place, commencing in early 2016 at two sites in Northern England where exploration was well advanced (see other papers in this thematic set for more detail). Development continued to be slow until hydraulic fracturing commenced in Lancashire in November 2018, allowing approximately 3 years of fixed site and 2.5 years of mobile survey baseline studies to be completed in advance of this activity, including during the period of well drilling.

Fixed location monitoring of greenhouse gases near to shale gas extraction gives some idea of the direction of the main sources upwind of the receptor site, but does not provide information on the nature of the sources or how many sources might be present in each wind direction footprint. Shale gas extraction often has a horizontal component, therefore possible emissions from this new source could also be mixed in with other emissions distal to the drill site. Given the need to locate, fingerprint and assess the footprint of existing sources influencing the region ahead of the potential addition of new sources from shale gas exploration, a series of measurement campaigns across a range of seasons and meteorological conditions has been carried out prior to the hydraulic fracturing process. These took place in 2 areas of planned development: 1. Preston New Road (PNR), Little Plumpton, Fylde, Lancashire and, 2. Kirby Misperton (KM), Ryedale, North Yorkshire. Fixed site measurements of greenhouse gases for this baseline project are discussed elsewhere (Fylde, Shaw et al., 2019; Ryedale, Purvis et al., 2019; Ward et al., 2017, 2018). The aim of the mobile study is to identify and characterise methane sources around these sites and assess seasonal variations in their distribution, so that any fugitive emissions to atmosphere added by unconventional gas extraction can be readily identified.

Previous studies show that large methane sources, such as landfill sites can still have a measurable contribution to ambient methane at considerable distances (4–5 km) downwind of the emission source (e.g. Lowry et al., 2001; Zazzeri et al., 2015), so the surveys were designed to cover a radius of at least 10 km from new unconventional gas operations. There have been numerous studies of fugitive methane emissions during shale gas extraction in the US, including ground-based (fixed and mobile) and aircraft measurement of gas emissions. Estimates of emissions vary widely. Particularly high emissions of 6.2%–11.7% of production were recorded over the Uintah basin in Utah (Karion et al., 2013), but measurements in some operational areas suggest leakage rates of closer to 1% of production (Peischl et al., 2015). US oil and gas methane emissions have been estimated to be 2.3% of production (Alvarez et al., 2018) and most emissions are from a small number of localities emitting large volumes of methane (Zavala-Araiza et al., 2015).

Given the small scale of unconventional gas operations in the complex UK landscapes with numerous and diverse sources, there is little potential for aircraft measurements to distinguish these sources at permitted flying levels. Although a total methane emission may be calculated under suitable meteorological conditions (e.g. O'Shea et al., 2014), the emissions from individual source categories are unlikely to be resolved. Ground surveys were considered the best option to locate and identify sources. Individual sources can be identified during ground-based methane surveys using continuous measurement of methane mole fraction by cavity-enhanced spectroscopy (eg. Rella et al., 2015a, Zazzeri et al., 2015; Boothroyd et al., 2016; 2017).

The National Atmospheric Emissions Inventory (NAEI) for the UK ([naei.beis.gov.uk/](http://naei.beis.gov.uk/)) provides a bottom up compilation of methane emissions by source category. The spatial resolution for most sources is  $1 \times 1$  km. Inventory maps were created for the two survey areas to provide potential survey targets for the early surveys (these are combined with source isotopic data in Section 4). Point sources represent a part of the inventory with defined emissions at individual high-resolution grid locations, which for the purposes of mapping become a contribution to the  $1 \times 1$  km grid square in which they are located. The NAEI inventory suggests that the main sources in a 10 km radius around both shale gas sites are dominated by animal husbandry, with additional emissions from nearby landfill sites and leaks from the gas distribution network (NAEI, 2019).

On the ground, the source distribution is often very different from inventory distribution. Landfill emissions are focussed toward the active cell, normally an area of  $400 \text{ m} \times 400 \text{ m}$  or less (e.g. Zazzeri et al., 2015), cow emissions are often focussed around barns (depending upon time of day and season), and gas leaks are located at infrastructure sources such as compressor stations, or along sections of old mains pipeline following major roads (e.g. von Fischer et al., 2017) rather than being distributed evenly around population centres.

Once emission plumes are located the sources need to be identified. Often the plume will occur directly next to a cow barn or a clearly marked landfill, or above ground gas infrastructure. Others such as gas network leaks do not have an obvious location, unless visible repair is ongoing. Similarly a manure pile could be hidden behind a high roadside hedge. Identification of such sources often requires another proxy. One of these is the carbon isotopic ratio of the methane ( $\delta^{13}\text{C}$ ). This works well in the UK for one main reason: the natural gas supply has a thermogenic source and so is enriched in  $^{13}\text{C}$  relative to ambient background air, which itself is enriched relative to the biogenic gas produced during waste degradation and by ruminant animals.

The database for isotopic signatures of methane, particularly  $\delta^{13}\text{C}$ , is increasing rapidly (Schweitzke et al., 2016; Sherwood et al., 2017).  $\delta^{13}\text{C}$  averages for aggregated source categories are: i) pyrogenic (biomass burning) averaging  $-22\text{‰}$  (range  $-35$  to  $-7\text{‰}$ ), ii) fossil fuels  $-44\text{‰}$  ( $-75$  to  $-25\text{‰}$ ), iii) microbial  $-62\text{‰}$  ( $-80$  to  $-40\text{‰}$ ). Each of these categories is further subdivided by region and activity, and each can be constrained often to a very small range within a local or regional survey area.

Some sources show consistencies even across continents: for example landfill sites (active  $-62$  to  $-56\text{‰}$ , closed  $-56$  to

**Table 1**

Literature values for C<sub>2</sub>:C<sub>1</sub> ratios of fossil fuels. In Summary: <0.005 is biogenic, >0.01 is thermogenic.

Source	C <sub>2</sub> H <sub>6</sub> :CH <sub>4</sub>	Reference
Oil Fields	0.15	Xiao et al. (2008)
Gas Fields	0.118	Rella et al. (2015b)
Thermogenic coal	0.1	Strapoć et al. (2007)
Gas Plants	0.08	Lopez et al. (2017)
Compressor Station	0.03	Lopez et al. (2017)
UK Gas Distribution	0.03	Xiao et al. (2008)
Biogenic Coal	0.005	Strapoć et al. (2007)

–52‰). Gas supply varies depending on source region (e.g. west Siberia  $-50 \pm 2\%$ , southern North Sea  $-31 \pm 2\%$ ; Lowry et al., 2001; Dlugokencky et al., 2011 and references therein), coal emissions vary between open-cast and deep mines and by rank from sub-bituminous to anthracite (Zazzeri et al., 2016), and waste processes in general (landfill, human and animal sewage) by the amount of oxygen present and the degree of oxidation taking place (eg. Liptay et al., 1998). Ruminant eructation emissions vary depending on diet (C<sub>3</sub> or C<sub>4</sub> diet) (Rust, 1981). Isotopic signatures for measured UK anthropogenic sources prior to this study are outlined in Zazzeri et al. (2015, 2017), following the earlier work of Hitchman et al. (1989) and Lowry et al. (2001). The range of  $\delta^{13}\text{C}$  ratios expected for the main UK anthropogenic sources varies from around  $-70\%$  for biogenic cow eructations to  $-25\%$  for combustion sources, such as vegetation fires.

Additional proxies can help with methane source identification, such as adding the D/H ratio measurement ( $\delta\text{D}$ ) to the carbon isotopes to resolve the sources in  $^{13}\text{C}$  vs  $^2\text{H}$  space (e.g. Röckmann et al., 2016). Additional gas species measurements can assist with identification of individual source categories, such as ethane for thermogenic gas or ammonia for animal wastes. The ratio of C<sub>2</sub>H<sub>6</sub>:CH<sub>4</sub> (hereafter simplified to C<sub>2</sub>:C<sub>1</sub> ratio) is widely used (e.g. Rella et al., 2015b) for surveys of fossil fuel production and distribution to separate pyrogenic and thermogenic (>0.03) from biogenic (<0.005) sources (Table 1).

## 2. Materials and methods

### 2.1. Mobile survey and sampling methodology

The Royal Holloway, University of London (hereafter RHUL) mobile laboratory has been operational since early 2013 and incor-

porates a Picarro G2301m (CO<sub>2</sub>, CH<sub>4</sub>, H<sub>2</sub>O) cavity ringdown spectrometer, sonic anemometer, GPS and inlet line for bag sampling (see Zazzeri et al., 2015 for details) with a Los Gatos Research (LGR) UMEA (Ultraportable Methane:Ethane Analyser) added in October 2017 (Fig. 1a and b). The addition of an ethane instrument allows quick identification of emissions from gas infrastructure or combustion. The delay time for instruments between air entering the inlet above the vehicle at 1.8 m and measurements being displayed is 7–9 s allowing for quick discovery and pinpointing of methane emissions. A Hemisphere GPS logs at 1 Hz (1 s) frequency and atmospheric measurements are offset to account for the lag between inlet and measurement. Instrument and computer times are synchronised at the start and end of daily surveys.

Eighteen 2-day campaigns were carried out before the start of hydraulic fracturing between March 2016 and October 2018 in the Fylde region and between October 2016 and March 2019 in the Ryedale region (Table S1). This format was considered to be the most efficient way to assess the change of sources with season (temperature, activity and location) under different wind speeds and directions. This strategy was for the most part successful with surveys carried out across the months June–November and January–March.

Survey periods generally lasted for  $\sim 7$  h from the time that the instruments were ready to measure. Routes were planned so that key source targets were surveyed on all days and this also included a circuit around the drill sites on the closest roads. Different routes were followed on the two days, so that most areas around the hydraulic fracturing site were covered during each survey period. This resulted in the identification of many additional sources that were revisited during subsequent campaigns. The survey coverage of each region is shown in Figs. S1 and S2.

Baseline driving speed was typically between 40 and 50 km/h. When emission plumes were encountered a repeat transect was driven at 20–30 km/h where traffic conditions permitted. This speed range has been identified (during field campaigns for the MEMO<sup>2</sup> project – see acknowledgements) as an optimum to maximise measurement points in a plume and to find a Gaussian peak shape for narrow point source peaks such as gas leaks or cow barns. If the excess methane in the peak was considered to be sufficient to potentially allow isotopic characterisation of the source to a high degree of precision (normally >200 ppb above the running background), then the vehicle was stopped and engine turned off for approximately 1 min in the centre of the plume, if traffic conditions permitted and it was safe to do so. This was sufficient



**Fig. 1.** a) Top: Picarro and LGR instruments plus battery power supply in the back of the RHUL vehicle, b) Mast on the vehicle roof with 3 air inlet lines, GPS and sonic anemometer to aid location of unidentified plumes.

time to fill a SKC Flexfoil bag (3 or 5 L volume) using a small KNF diaphragm pump with sufficient air to measure both the mole fraction (1 L) and carbon isotopes (0.3 L) to high precision once back in the RHUL laboratory.

Wider emission peaks such as from landfill sites or large above-ground gas infrastructure could be sampled at multiple points in the plume at different levels of excess mole fraction over background, which allowed more precise characterisation of the source isotopic signature. Wider emission plumes could also be sampled while the vehicle was moving, if it was in the plume for more than the 30–40 s required to fill the bag. Ideally plumes were intersected perpendicular to the wind direction to give the best peak shapes.

In some places there were multiple sources in close proximity. In these cases the separation of plumes required a very specific wind direction and moderate but constant wind speeds with low turbulence to sample individual emission plumes. This can be seen most clearly in the adjacent sources to the east of the site at Little Plumpton where gas leaks and cow barn are close to each other (discussed later in Section 3).

The isotopic source characterisation requires that a stable background methane mole fraction can be measured, sampled and subtracted from the peaks. The bottom 2% of methane mole fractions measured were within  $\pm 7$  ppb for most days without atmospheric inversion conditions, and this daily background could be used for source calculations of all plume samples. Typically background bag samples were collected away from the influence of local sources at the beginning and end of the day. Under inversion break-up conditions, where the methane background can be continually reducing throughout the survey, a background air sample was collected upwind or adjacent to every major plume that was sampled.

## 2.2. Laboratory analysis

Mobile survey instruments were calibrated to the WMO X2004A CH<sub>4</sub> scale in the RHUL Greenhouse Gas laboratory between campaigns using cylinders of air filled and measured by NOAA and tertiary standard cylinders filled and calibrated against the NOAA scale by MPI Jena. The LGR UMEA instrument was additionally calibrated using 2 cylinders with known C<sub>2</sub>H<sub>6</sub> as well as an in-house determined temperature correction.

The Flexfoil bag samples were analysed for methane mole fraction and  $\delta^{13}\text{C}$  at RHUL. Methane mole fractions were analysed using a Picarro 1301 cavity ringdown spectrometer with a reproducibility of  $\pm 0.3$  ppb. For isotopic analysis the samples were analysed in triplicate using continuous-flow isotope ratio mass spectrometry (CF-GC-IRMS – Elementar Trace Gas module and IsoPrime mass spectrometer). The mean repeatability of  $\delta^{13}\text{C}$  measurements is 0.05‰. This technique is described by Fisher et al., (2006) and summarised for mobile campaign samples by Zazzeri et al. (2015).

## 2.3. Data processing of mobile measurements

Raw data for each survey were calibration corrected, and additionally time corrected for inlet lag to match as perfectly as possible the location measurements with greenhouse gas measurements.

The “background” mole fraction of methane was defined as the lowest 2nd percentile from a  $\pm 10$  min moving average, thus allowing the defined background to vary as the background conditions evolve over the day and vary spatially across the survey route. The background was then subtracted from each measurement to give “excess methane over background”. Any data points where the background value of methane is higher than 2 ppm are filtered

out as these conditions are not representative of normal background mole fractions and are likely to represent build-up of methane under inversion conditions, giving rise to anomalously high mole fractions around points of emission and plume merging.

Each survey gives a snapshot of the methane emissions as the vehicle makes each downwind pass, and combining all of the surveys can begin to build a picture of the average reach of various methane sources. However, some routes were surveyed more frequently and this bias needs to be accounted for. In order to achieve this, the CH<sub>4</sub> point data from all surveys have been averaged into  $10 \times 10$  m bins and these averaged into  $100 \times 100$  m bins (and then into 1 km<sup>2</sup> bins for NAEI comparison). The underlying concept is that the resulting map will show areas that are most impacted at vehicle inlet height by sources of methane and gives an estimate of emission consistency for the very frequently surveyed roads. The most prevalent wind directions will be captured more often by the surveys, and therefore the final result should capture a realistic impact of the prevailing wind. A graphical representation of the binning process is shown in Fig. S3.

Data from the LGR UMEA have been collated to produce C2:C1 plots as shown in Figs. S4 and S5. To produce the overview plots, the data were filtered to include only points where there are enhancements of ethane > 50 ppb or methane > 200 ppb above the background mole fraction for 10 consecutive data points. These data are then plotted on maps as a moving 10-second average C2:C1 ratio. This removes the possibility of peak misidentification caused by fluctuations in instrument noise (instrument precision is 30 ppb (1 $\sigma$ , 1 s) for ethane). Selected sections of interest from these maps are shown as a data layer on many of the figures to demonstrate the ability and consistency of using a C2:C1 tracer map as both complementary, and as an alternative, to spot sampling for isotopes, when the only requirement is to distinguish pyrogenic, thermogenic and biogenic sources.

## 2.4. Data processing of isotopic measurements

The use of carbon isotopes to distinguish methane sources is a well established technique and the procedure used by the RHUL group has been outlined in detail elsewhere (Zazzeri et al., 2015, 2017; France et al., 2016).  $\delta^{13}\text{C}$  data for atmospheric samples are used to calculate a  $\delta^{13}\text{C}$  source signature for each individual or groups of like plumes sampled on the same day using Keeling plot analysis (eg. Keeling, 1961; Lowry et al., 2001; Pataki et al., 2003; Zazzeri et al., 2015). This requires that samples of background air, with no influence (atmospheric contribution) from the source being investigated (or other neighbouring sources) are collected to provide one end member to the Keeling plot. The other sample points in the plume represent mixing between this background and an unknown source, the signature of which can be calculated as the y-axis intercept of  $\delta^{13}\text{C}$  vs  $1/\text{CH}_4$  (see Pataki et al., 2003; Zazzeri et al., 2015, for details of how these calculations are made). These plots were produced for interim reports of the BEIS project (see Ward et al., 2017, 2018), but are not included here.

The isotopic data for a single campaign (including those collected under strong inversion conditions) can be analysed in isolation using the Keeling plot approach to give interesting and relevant data (such as seasonal variability of animal husbandry). However, it is also useful to consider the dataset as a whole to generate isotopic maps that are representative of the full baseline period. In order to combine isotopic data points for an individual source from many surveys, re-analysis using the Miller-Tans method (Miller and Tans, 2003) is required. This method requires assignment of seasonal (moving) background  $\delta^{13}\text{C}$  and mole fraction values to each elevated methane spot sample. The background points were allocated manually using surveying and analysis notes. New isotopic datasets covering all surveys were then created based

upon both geographic data and location notes to create datasets where the same methane source was sampled during multiple surveys. The resulting datasets for each methane source were plotted as Miller-Tans plots (see Fig. S6 for examples), where the slope of the linear regression represents the source  $\delta^{13}\text{C}_{\text{CH}_4}$  signature (Miller and Tans, 2003; Zazzeri et al., 2017).

### 3. Survey results and source identification

#### 3.1. Summary of results and identified sources

The survey datasets for each region have been combined as excess over background maps to simplify data presentation (see Section 2.3 above). Each survey alone can identify sources as a single snapshot in time (Fig. 2) and provide a framework for sample collection, but does not allow for the changing meteorology and movement of ephemeral sources (such as manure piles). The locations of the identified main methane sources are shown in Fig. 3 (Fylde) and Fig. 4 (Ryedale), colour coded by their calculated mean isotopic signatures. Fugitive gas leaks, landfill sites and agricultural sources can be clearly discriminated by their  $\delta^{13}\text{C}_{\text{CH}_4}$  signatures. Drilling sites in both regions are located close to barns that house dairy cattle during the winter and at milking times at other periods of year when the weather is warmer and grass supply sufficient. These are a major source of methane that needs to be distinguished from any potential emissions from the unconventional gas extraction process.

The dominant wind directions recorded at the PNR (Preston New Road) fixed monitoring site, Fylde, are from the SW to WNW sector (225–285°, Fig. 5a). At the KM (Kirby Misperton) Ryedale site there is a wider field of dominant westerlies (195–325°, Fig. 5b). Ryedale shows similar methane distribution for all wind directions. By comparison Preston New Road suggests a predominance of close sources in the NE to SE sector (see Shaw et al., 2019, and Section 3.1 below). The higher  $\text{CH}_4$  mole fractions are due to the close proximity of a farm source to the fixed measurement site.

The C2:C1 data plots for the campaigns FY4-FY9 and KM4-KM9 are shown in Figs. S4 and S5. These highlight the dominant trends observed during the baseline period. Fig. 6 shows selected peaks from the FY6 survey in February 2018. Infrequent combustion sources are clearly distinguished by a C2:C1 ratio normally >0.2, while the biogenic sources (farms, landfills) are <0.005. Between these are the fugitive fossil fuel emissions. The two gas leaks in Fig. 6 have ratios of 0.055 to 0.065, but the total range encountered is from 0.045 to 0.09. It is possible that the 0.045 ratio represents a mixed plume from a biogenic and a thermogenic source, as there are adjacent farms and gas leaks in the survey areas.

#### 3.2. Fylde, Lancashire

##### 3.2.1. Mobile survey sources

The main sources located within a 10 km radius of the PNR site are cow eructations and cow manure (both combined in cow

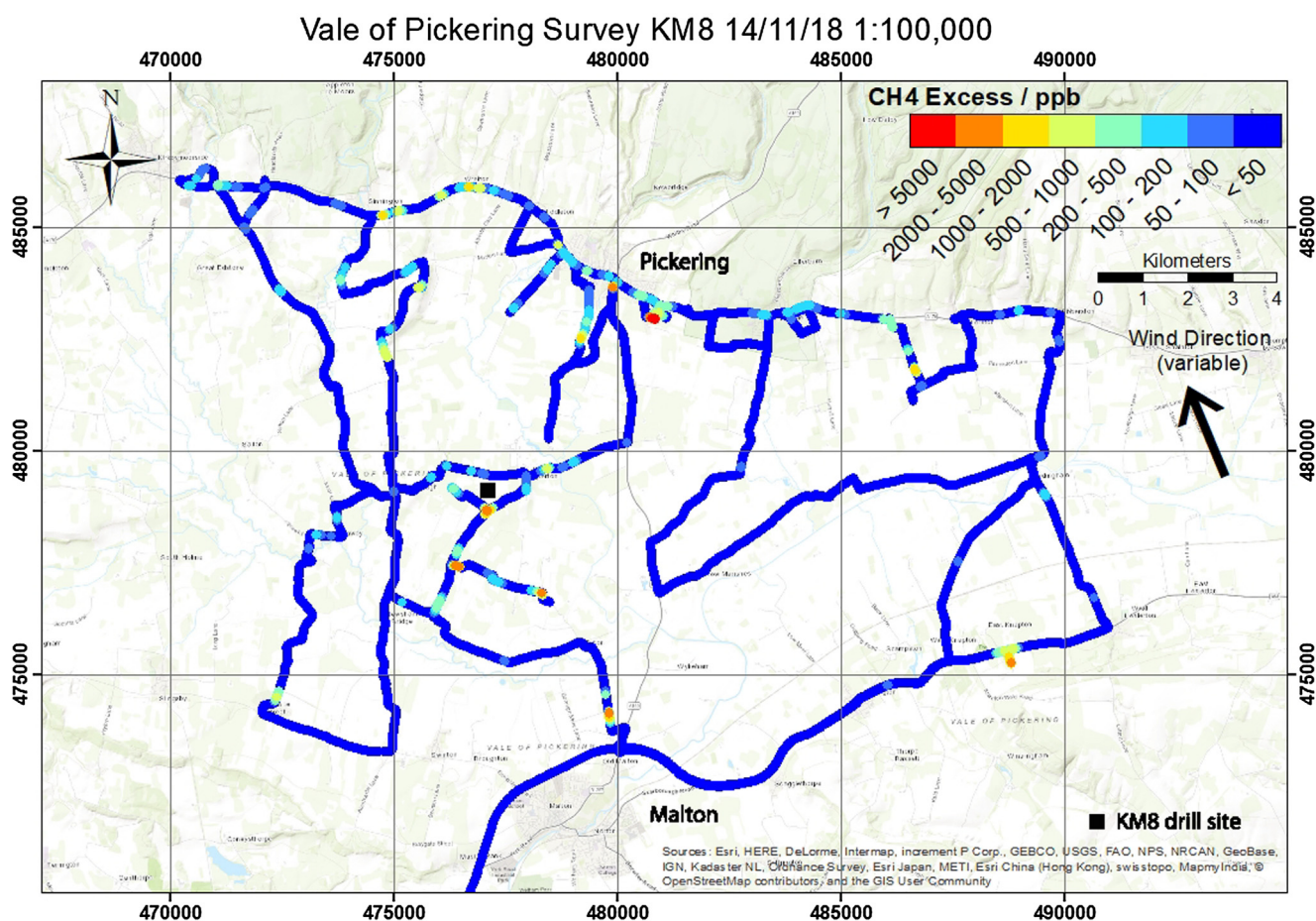


**Fig. 2.** Example of a 1-day survey route, representing 6–7 h of survey time following instrument warm-up. This example is for Ryedale on November 14, 2018. The methane is colour-coded by excess over background, with the deep red hotspot in the north of the map being a gas offtake station, and the orange hotspot to the SE being a landfill site. The black square is the site of drilling. Base map provided by © OpenStreetMap contributors. (For interpretation of the references to colour in this figure legend, the reader is referred to the web version of this article.)

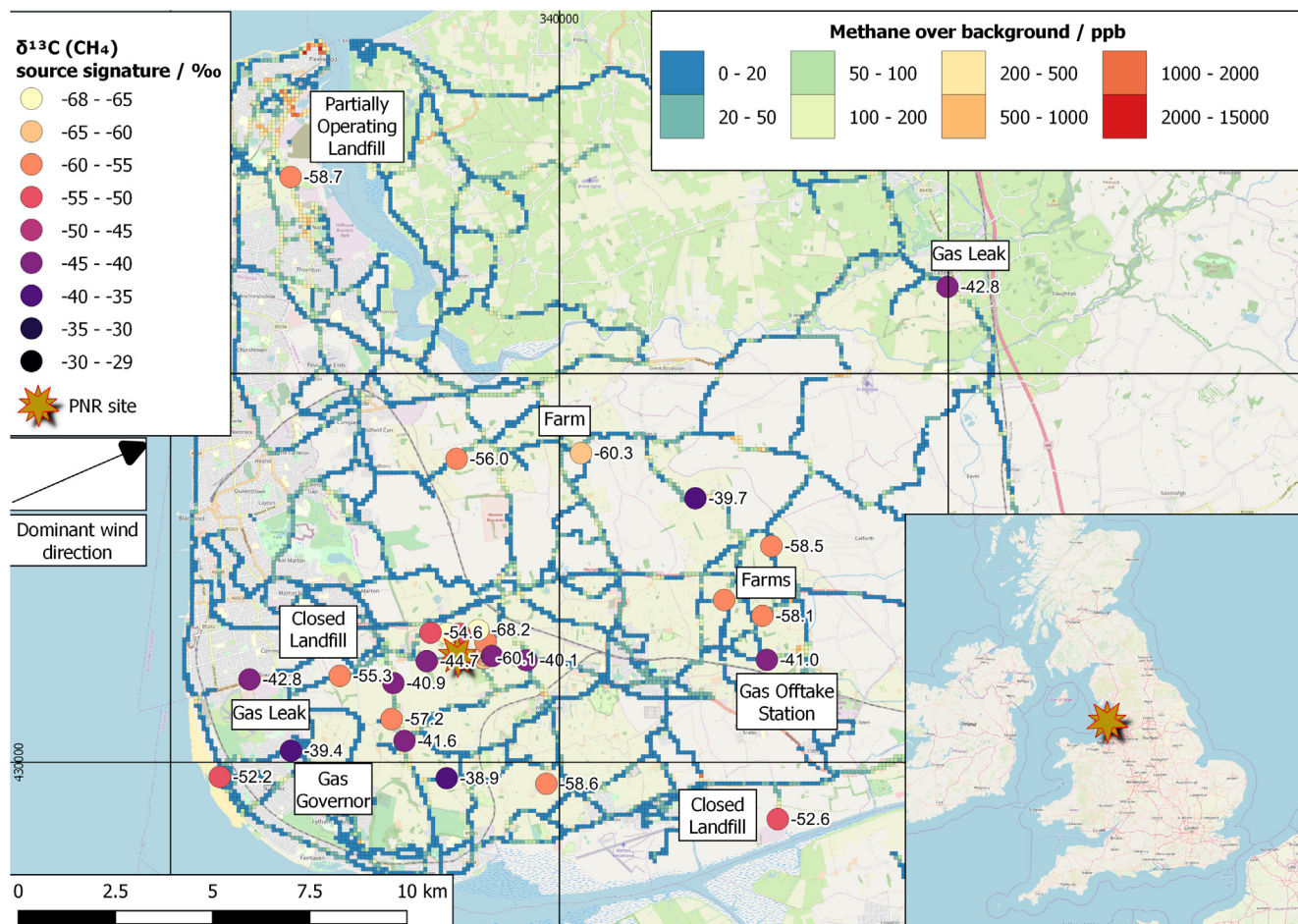


**Fig. 3.** Summary map of Fylde combining data from 9 surveys, with each source located as a circle and superimposed on the  $100 \times 100$  m grid of average methane excess. These are colour coded by isotopic ratio from most biogenic (yellow) to most thermogenic (black) with the mean Miller-Tans  $\delta^{13}\text{C}$  signature across all surveys highlighted. Base map provided by © OpenStreetMap contributors. (For interpretation of the references to colour in this figure legend, the reader is referred to the web version of this article.)

barns), landfill sites, and gas leaks from above ground infrastructure and below ground pipework (Figs. 3, 7 and 8). While the above ground gas escapes directly to atmosphere, the below ground emissions are either from holes (during pipe replacement), through soil or road surfaces, or through storm drains, the latter representing the largest measured mole fractions from underground sources. Gas emissions have been identified from a gas offtake station 8 km E of the PNR site, a gas governor in a suburb 3 km to the SW (both associated with pressure reduction), and regularly from underground on 3 roads: Preston New Road that runs along the south side of the PNR site, Peel Road running N-S. 1.5 km SW of the drill site but likely an influence on continuous PNR measurements under inversion conditions, and on Peg's Lane, 3 km south of the site. Closed landfill sites 13 km to the NNW and 9 km to the SE are too far away to influence continuous measurements adjacent to the PNR site, but a restored landfill 3 km W will be an influence under inversion conditions. Cows are located widely across the sphere of influence of the PNR site, as suggested by the NAEI inventory. As well as a dairy farm next to the PNR site, there are at least 3 farms within 3 km of the site that are regular emitters of  $\text{CH}_4$ .

The circuit road around the drilling pad is between 200 and 1000 m from the site (Fig. 9). Sources encountered on this circuit alone are farms (cow barns) to the NW and E, a manure pile to the N (seasonal), cows in fields to the NE (seasonal), and gas leaks (including once during pipeline replacement) along Preston New Road (the southern perimeter between ESE and WSW of the site).

### 3.2.2. Isotopic signatures

Summary Table 2 highlights the differences of  $\delta^{13}\text{C}$  signatures for the main sources identified during the surveys. Gas leaks are consistently enriched relative to atmospheric background ( $-48$  to  $-47.5\text{‰}$ ), ranging from  $-44$  to  $-39\text{‰}$  for individual gas leak sources. All other sources are depleted in  $^{13}\text{C}$  relative to atmospheric background, the closest being manure piles (commonly  $-52$  to  $-50\text{‰}$ ). Measurement of methane in cow breath when the animals were directly behind a gate gave  $\delta^{13}\text{C}$  source signatures of  $-71$  to  $-67\text{‰}$ . When the cows were inside the barns the signatures measured for the emission plumes emanating from the barns varied greatly in the range  $-66$  to  $-56\text{‰}$ . Although the cows in the barn could not be counted or the status of the waste be assessed it is presumed that the wide signal goes from one dominated by cow breath in a clean barn (more depleted  $^{13}\text{C}$ ) to few cows in a barn not cleaned of animal waste (less depleted  $^{13}\text{C}$ ). Signatures from landfill sites vary from  $-61$  to  $-53\text{‰}$  and overlap with both cow barns and manure piles, but can be subdivided into closed landfill sites where residual methane is undergoing some subsurface oxidation before emission ( $-56$  to  $-53\text{‰}$ ) and active landfill sites with emission from active cells / gas extraction pipes. There is a much larger emission from uncovered active cells ( $-61$  to  $-57\text{‰}$ ) that swamps the signal from topsoil oxidation of older cells. Different source types are occasionally adjacent in location. Where cows are grazing next to a closed landfill the cow breath ( $-70\text{‰}$ ) is quite distinct from the landfill ( $-54\text{‰}$ ).

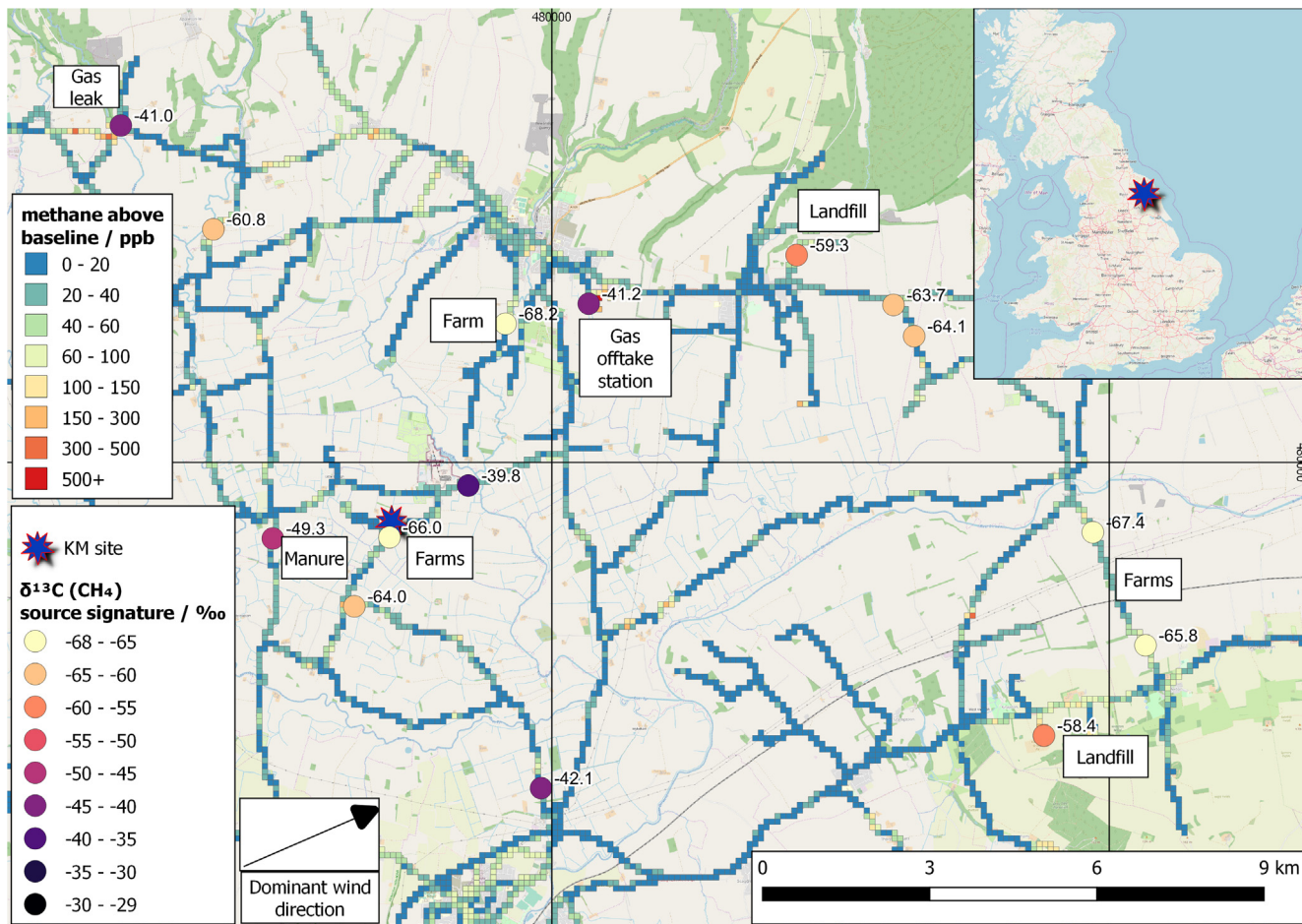


**Fig. 4.** Summary map of Ryedale combining data from 9 surveys, with each source located as a circle and superimposed on the 100 × 100 m grid of average methane excess. These are colour coded by isotopic ratio from most biogenic (yellow) to most thermogenic (black) with the mean  $\delta^{13}\text{C}$  signature across all surveys highlighted. Base map provided by © OpenStreetMap contributors. (For interpretation of the references to colour in this figure legend, the reader is referred to the web version of this article.)

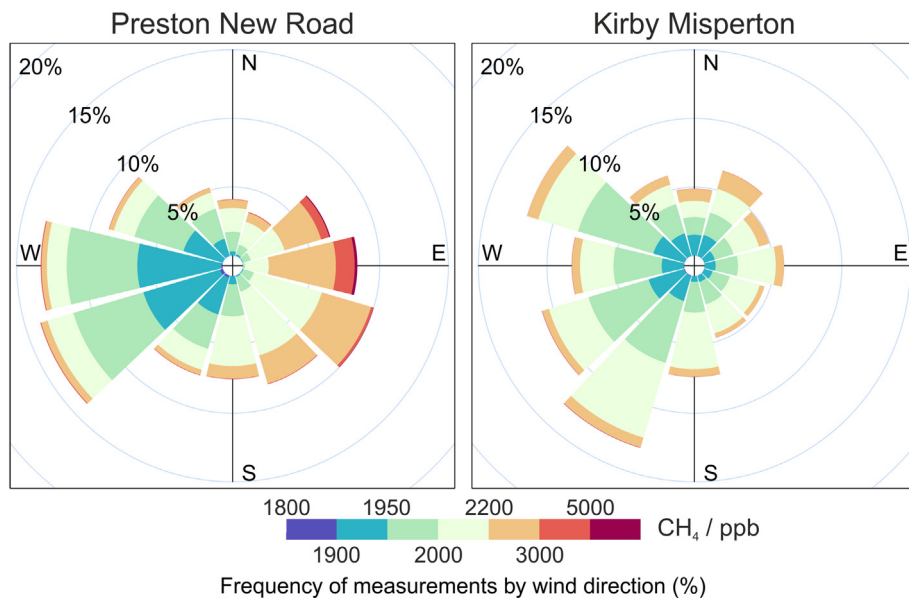


**Fig. 5.** Wind roses for the period March 2016 to March 2019, which encompasses all of the mobile surveys in both a) Fylde and b) Ryedale.

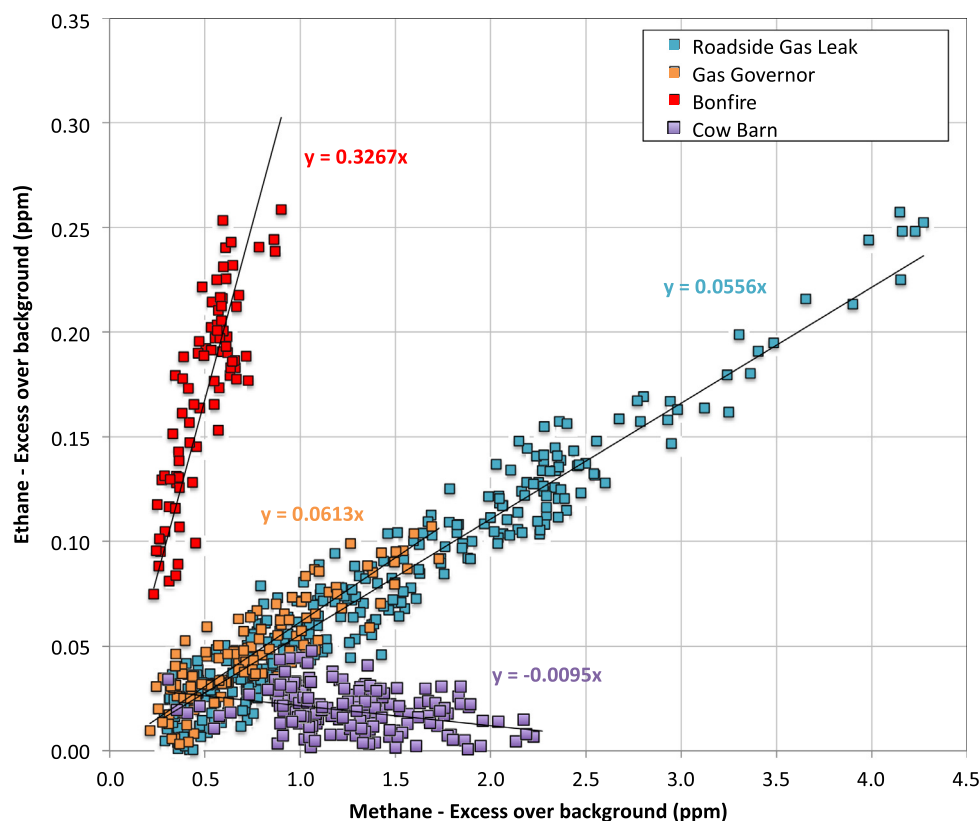


**Fig. 6.** Ethane vs methane for individual sources measured during the FY6 campaign using the Los Gatos UMEA instrument. Data are filtered to only include points where  $\text{CH}_4$  excess is  $>250$  ppb. Three distinct trends stand out;  $\text{C}_2:\text{C}_1 < 0.01$  (purple) is for a cow barn and any ethane measured is within baseline noise,  $\text{C}_2:\text{C}_1$  between 0.055 and 0.065 (blue and orange) are for two thermogenic gas sources, and  $\text{C}_2:\text{C}_1 > 0.2$ , (red) showing strongly enhanced ethane that is emitted by a bonfire burning wood products. All biogenic sources measured have  $\text{C}_2:\text{C}_1$  ratios  $< 0.01$ . (For interpretation of the references to colour in this figure legend, the reader is referred to the web version of this article.)

### 3.2.3. Ethane:Methane ratios

Ethane was measured in campaigns FY4 to FY9. Fig. 6 highlights the observed difference in ratio trends between gas pipe leaks, bonfires (combustion) and the biogenic sources. The continuous nature of the  $\text{C}_2:\text{C}_1$  data set is especially useful where plumes of methane of differing provenance merge into each other, such as the farm and gas leak in the SE corner of Fig. 9. When the wind direction means that the survey path is perpendicular to both sources then the mixed ratio in the zone of plume overlap is very small (Fig. 9), but there will be more mixing of plumes under less ideal meteorological conditions. The merging of plumes is seen also between a gas leak and landfill on Peel Road (Fig. 8) and between a gas offtake station and local farm (Fig. S7), 8 km east of PNR site. Ratios of  $\text{C}_2:\text{C}_1$  for clearly separated individual plumes are between 0.055 and 0.075 for all gas supply leaks in the Fylde region. For farm and landfill sources these are  $< 0.005$ .

## 3.3. Ryedale, Yorkshire

### 3.3.1. Mobile survey sources

The main sources located within a 10 km radius of the KM site are similar to those in Lancashire, being cow eructations and cow manure (both combined in cow barns), landfill sites and gas leaks from above ground infrastructure and below ground pipework (Figs. 4 and 10). The circuit around the KM drilling site reveals cow barns, manure piles and a persistent gas leak to be the main methane sources within 2 km, and only one cow barn is within 500 m. The main persistent natural gas source is a gas offtake station 6 km NE of the KM site (see Fig. S8). Plumes from this source were encountered during all 9 surveys and only on 2 individual

days with WNW-NW winds was the closest downwind road too far away to detect the plume ( $>2$  km). Other gas leaks, such as along the main road between Pickering and Kirbymoorside, on Edenhouse/Riggs Road north of Malton, and east of Kirby Misperton village, were from roadside ditches or culverts, and not measured (or not surveyed) during all campaigns. Landfill sites were at a significant distance from the KM site. A landfill site 13 km ESE of the KM site was the main methane source in the region and a continual emitter, although activity on the site had ceased by March 2019 and a significant reduction in measured peak height was observed directly downwind of the site (to 10–20% of previous surveys).

### 3.3.2. Isotopic signatures

$\delta^{13}\text{C}_{\text{CH}_4}$  signatures of the main sources are very close to those found in the Fylde region (Table 3). Gas leaks and the gas offtake station are consistently enriched relative to atmospheric background, with  $\delta^{13}\text{C}$  ranging from  $-42$  to  $-40\text{‰}$  for individual gas leak sources, a narrower range than Fylde, but similar to signatures of  $-38 \pm 3\text{‰}$  previously reported for gas pipelines in the Pickering area (Boothroyd et al., 2018). All other sources are depleted in  $^{13}\text{C}$  relative to atmospheric background, the closest being manure piles (ranging from  $-57$  to  $-50\text{‰}$ ). Cows were more often in barns compared to in the Fylde so eructations were not directly sampled. Cow barn signatures varied between  $-67$  and  $-59\text{‰}$ , slightly more depleted in  $^{13}\text{C}$  on average than the Fylde barns. During the November 2018 Ryedale survey enough sheep were clustered together to produce a significant  $\text{CH}_4$  plume allowing a source signature of  $-60\text{‰}$  to be calculated.

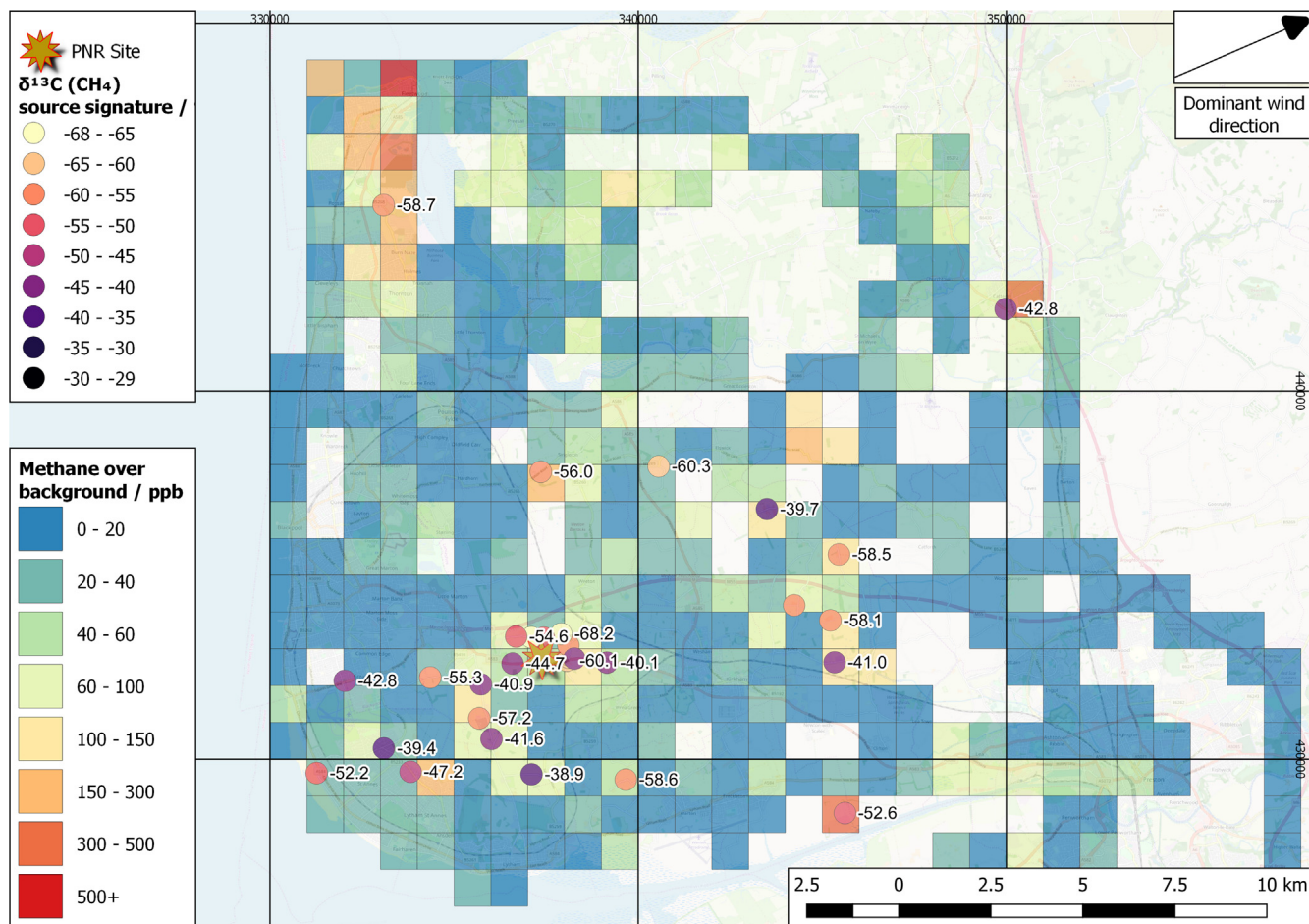


**Fig. 7.** Excess over background averaged by  $1 \times 1$  km grid squares for all squares visited at least twice during the 9 Fylde surveys. Sources sampled and their averaged isotopic signatures across the surveys are shown. Base map provided by © OpenStreetMap contributors.

The isotopic signature of landfill emissions from the site 13 km to the SE ranged from  $-61$  to  $-59\%$  when active, but changed to  $-56\%$  for the final survey, more typical of signatures for covered cells. Emission plumes from another closed landfill site 9 km NE of the KM site were identified in some surveys and had a signature of  $-57 \pm 1\%$ .

### 3.3.3. Ethane:Methane ratios

These ratios clearly distinguish between the agricultural and the gas supply network sources, as in the Fylde region (Fig. S9). The offtake station and three roads with gas leaks had C2:C1 ratios mostly between 0.07 and 0.08, the farming sources  $<0.005$ . Two combustion sources were identified, one a narrow plume from a bonfire, the other from driving downwind of the exhaust of an old vehicle in the town centre of Pickering. The combustion sources have significantly higher C2:C1 ratios of up to 0.82. For sources that are close to the KM drilling site, the cow barns and manure piles are clearly distinguished from the gas leak to the east of Kirby Misperton village (Fig. 11).

## 4. Discussion of the wider implications of the survey results

### 4.1. Distance for plume detection

The changing wind direction at UK sites often requires multiple surveys under different atmospheric conditions to locate and assess the sphere of influence of known sources and identify non-inventory sources. The excess over background for each

source type is largest at the closest monitoring point to the source, if the source is at ground level. The largest sphere of influence of sources in the baseline surveys is from landfill sites and gas offtake stations, but these are far enough away that they do not contribute to the methane measured at the continuous measurement sites adjacent to the drill sites. While observed influence can reach 1.5 km during daytime surveys, their influence could extend further under nighttime inversion conditions, but when multiple sources are present in a region their emissions tend to merge and mix under the inversion, so that the contribution from each cannot be quantified.

Cow barns, manure piles and gas leaks are the sources that contribute to peaks observed at the continuous monitoring sites during the baseline period at both FY and KM. These sources have  $\delta^{13}\text{C}$  signatures close to  $-60$ ,  $-50$  and  $-40\%$ , respectively. As the farm sources have no ethane, the C2:C1 ratios will at least give an estimate of the proportions of gas leak to farming sources.

In summary the influence of each plume varies with emission rate and area of each source:

- The largest high emitting area sources are active landfill cells, with statistically significant excess over background recorded up to 5 km downwind from site for the larger landfill operations, but up to 1.5 km in the surveyed regions. Some larger gas infrastructure, such as offtake stations, have plumes that can be identified 1–1.5 km downwind (Fig. S8).
- More focused plumes such as cow barns or biogas plant plumes have influence to around 500 m downwind of source.

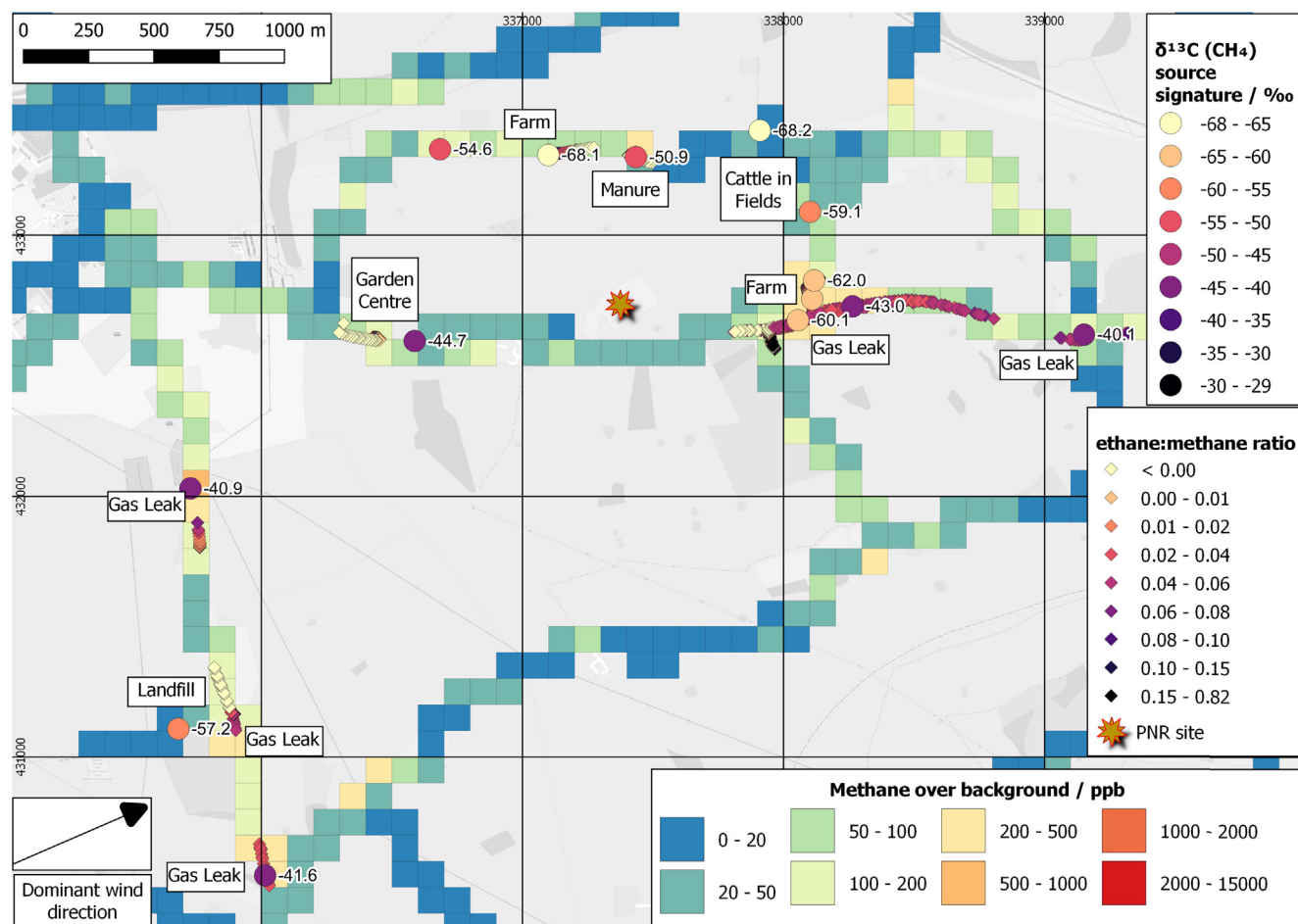


**Fig. 8.** Zoomed in maps around the PNR drilling site: Continuous monitoring of methane and meteorological parameters by the University of Manchester is between the shale gas site and the farm to the east (see Shaw et al., 2019). The figure shows the averaged methane during all 9 surveys for  $100 \times 100$  m boxes overlain by C2:C1 ratio traces and isolates the high (gas leak) and low (biogenic) C2:C1 ratios, with the isotopic signatures for identified sources for comparison. Base map provided by © OpenStreetMap contributors.

- Roadside point source gas leaks vary from 10 s to 100 s of metres depending on emission rate and wind speed. Manure piles are similar.
- A plume from a dispersed field of cows is significant only for 100 s of metres.

#### 4.2. Seasonal source variation

No seasonal variations have been observed in the position of plumes or the isotopic signatures of gas leaks or landfill sources. The main differences are in the agricultural sources, with the appearance of manure piles in March, which persist for much of the spring and summer, and the dispersion of ruminants across fields. The timing of these events varies greatly due to the inconsistency of the British weather. When the cows are in the fields and the manure piles in discreet corners it is possible to identify 2 isotopic end members for the agricultural source, the eructations at  $-70\text{‰}$  and the manure piles close to  $-50\text{‰}$ . The very dry late spring and summer of 2018 caused some inconsistencies in this ideal, with manure drying out and reports of animal dietary supplements with a C4 plant component such as maize (substantially more enriched in  $^{13}\text{C}$  than grass). It is also highly likely that diets are supplemented with C4 components during the winter months causing  $^{13}\text{C}$ -enrichment in the breath component of the barn  $\text{CH}_4$  signature.

#### 4.3. Temporal source changes

Some sources change with time, others are ephemeral. This has included change of activity or closure of landfill sites, associated with a reduction in the emissions. Evidence for this comes from much lower downwind peak height during surveys undertaken in similar meteorological conditions, with a correlated relative enrichment in  $^{13}\text{C}$ , normally associated with an increase in oxidation once the active cells are capped.

Visually the number of sheep encountered in fields in the Ryedale area was higher from the second part of 2018 onwards, so much so that an isotopically distinct sheep emission plume could be measured at one location ( $\delta^{13}\text{C}$  of  $-60\text{‰}$ ).

Larger gas leaks tend not to persist, because they are reported and fixed, or they may occur during the process of planned pipe-work replacement. Smaller peaks, normally 1–3 ppm above background can often persist. These would not be detected by the mercaptan ( $\text{CH}_4\text{S}$ ) smell at these levels and may be uneconomical to fix. Examples in this category have been measured across the whole survey period, when wind directions are favourable, meaning that they were not measured in all surveys.

#### 4.4. Proxies for source identification

Many sources can be identified by using maps directly, such as cow barns or landfills. Some are already included in the NAEI. For

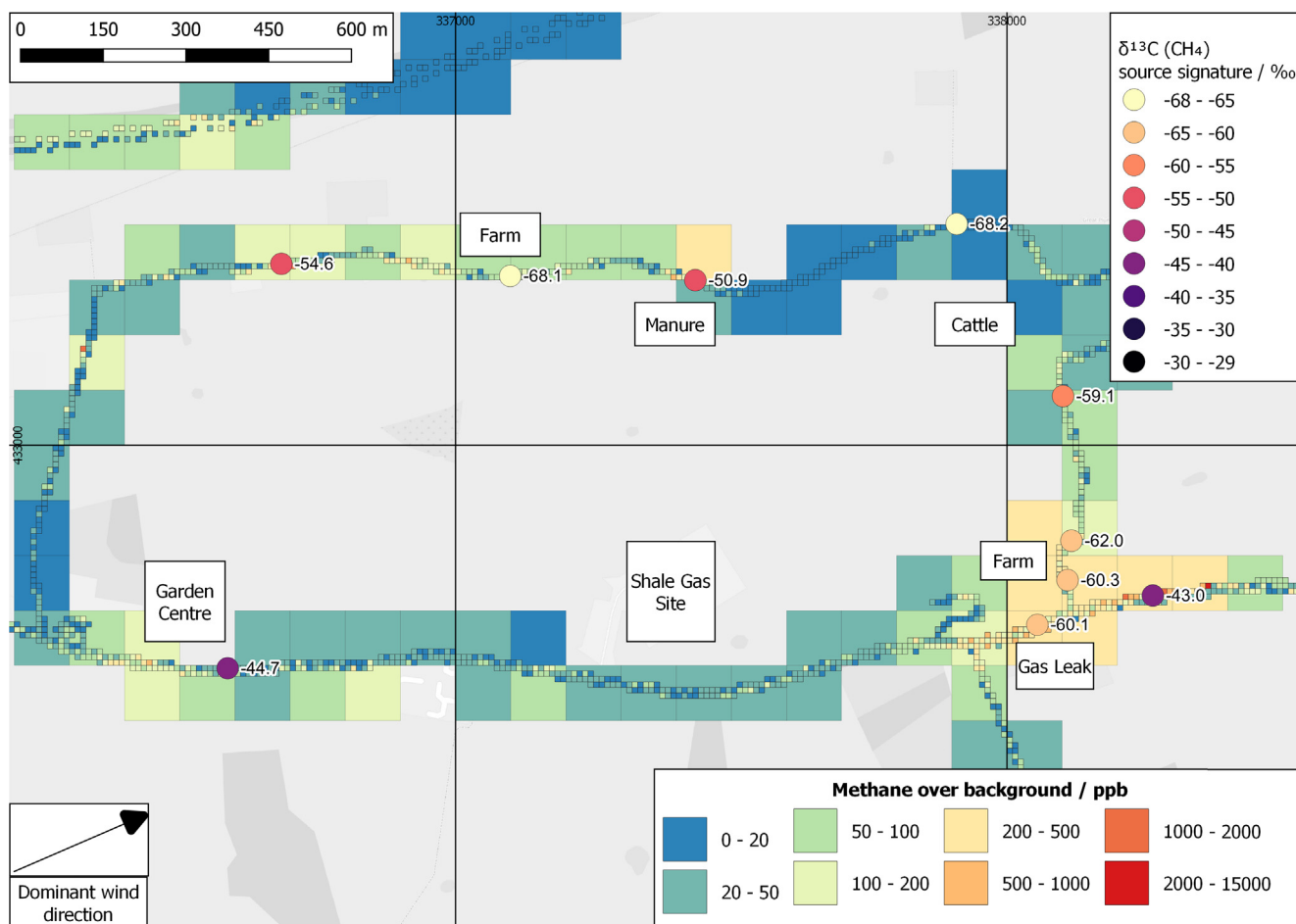


**Fig. 9.** Zoomed in image of the road circuit around the PNR drilling site (centre bottom) showing the main sources and their isotopic signatures, and the excess methane during all 9 surveys aggregated by  $10 \times 10$  and  $100 \times 100$  m grid squares (see Fig. S3 for how the different aggregations are created). Farm signatures are close to  $-60\%$ , manure piles  $-50\%$  and gas leaks  $-40\%$ . Base map provided by © OpenStreetMap contributors.

**Table 2**

$\delta^{13}\text{C}$  signatures of the main methane sources seen on each campaign in the Fylde region identified from Keeling plot analysis. The month that each survey was performed is also listed.

Source	Number	$\text{CH}_4$ $\delta^{13}\text{C}$ signature (‰)										Mean $\pm 1 \sigma$
		FY1 03/16	FY2 07/16	FY3 06/17	FY4 10/17	FY5 01/18	FY6 02/18	FY7 07/18	FY8 08/18	FY9 10/18		
Dairy farms	Many	$-60.2$ – $64.4^b$	$-58.4$	$-59.1$	$-60.9$	$-66.2$	$-61.0$	$-62.7$	$-59.1$ – $67.9^b$	$-62.9$	$-61 \pm 2$	
Manure piles	Many	$-51.6$		$-53.1$		$-58.6$		$-55.9$	$-51.6$		$-54 \pm 3$	
Gas leaks	Many	$-41.2$		$-40.9$	$-42.8$	$-42.6$	$-40.6$	$-40.8$	$-40.5$	$-39.4$	$-41 \pm 1$	
Closed Landfill	3	$-55.1$				$-55.5$		$-55.8$		$-54.3$	$-55 \pm 1$	
Active Landfill	1	$-57.8$	$-58.4$	$-58.3$			$-59.8$	$-58.7$			$-59 \pm 1$	

these the isotopes measurements provide a method to isotopically characterise the source category. Many smaller sources are identified only during mobile surveying. Addition of ethane measurement allows quick identification of fugitive emissions from the gas supply network, and of the few significant combustion sources, during the mobile surveys. In a similar way laser-based methane carbon isotope instruments can separate biogenic from thermogenic sources during surveys (eg. Phillips et al., 2013). Only the laboratory-based high precision carbon isotopic analysis is successful in unpicking the isotopic complexities of the biological sources. These are largely controlled by oxygen content (aerobic vs anaerobic) and diet, which during the survey period were strongly influenced by the rainfall in the survey regions.

The C2:C1 ratios also might add distinction between gas networks. The C2:C1 ratios for the Ryedale gas network are more con-

sistent and on average higher than for the Fylde region, but there are no observed overlapping gas and farm sources. While the difference in ratio might be partially down to mixing with biogenic sources in the Fylde, it could represent difference in composition of supplied gas between NE and NW England and this needs further investigation. The combination of 1 Hz ethane measurement with high-precision  $\delta^{13}\text{C}$  data has so far proved to be a successful combination (eg. Figs. 8 and 11).

#### 4.5. Spatial comparison with NAEI emission inventory

The excess over background mapped on the  $1 \times 1$  km grid for both survey areas (Figs. 7 and 10) shows a very different spatial distribution to the NAEI inventory. Fig. 12 gives the example of the 2016 NAEI methane inventory mapped by  $1 \times 1$  km grid square

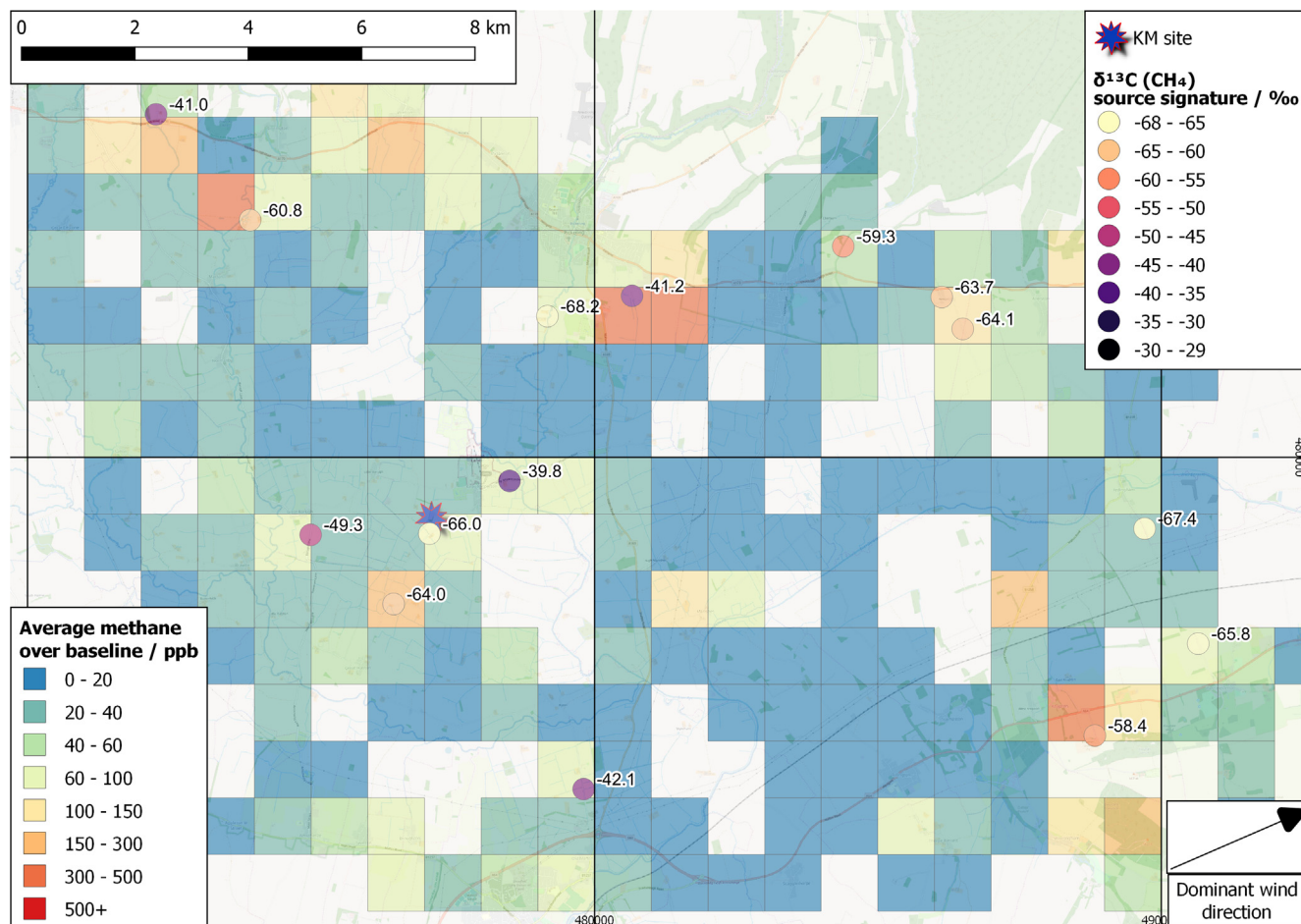


**Fig. 10.** Excess over background averaged by  $1 \times 1$  km grid squares for all squares visited at least twice during the 9 Ryedale surveys. Sources sampled and their averaged isotopic signatures across the surveys are shown. Base map provided by © OpenStreetMap contributors.

**Table 3**  
 $\delta^{13}\text{C}$  signatures of the main methane sources seen on each campaign in the Ryedale region identified from Keeling plot analysis. The month that each survey was performed is also listed.

Source	Number	$\text{CH}_4$ $\delta^{13}\text{C}$ signature (‰)										Mean $\pm 1 \sigma$
		KM1 10/16	KM2 01/17	KM3 06/17	KM4 10/17	KM5 01/18	KM6 03/18	KM7 07/18	KM8 11/18	KM9 03/19		
Dairy farms	Many	-63.6	-59.3	-64.7	-66.2	-67.3	-65.5	-67.0	-64.1	-63.9	-65 ± 2	
Manure piles	Many			-49.7	-56.7		-50.1			-51.2	-52 ± 3	
Sheep	Many								-59.7		-60	
Gas offtake station	1	-41.7	-42.4	-40.6	-42.9	-42.0	-42.0	-41.9	-41.2	-41.4–40.4	-42 ± 1	
Gas leaks	4			-39.9	-41.4	-41.5	-41.6		-42.0		-42 ± 1	
Landfill (closed)	1	-57.4	-57.3				-57.9			-56.2	-57 ± 1	
Landfill (active)*	1			-58.5	-58.6	-59.6	-61.1	-58.7	-61.4		-60 ± 1	

for the Fylde region. The dominant source is the broadly distributed dairy farming source in rural areas and the gas distribution network in urban areas, with localised hotspots for landfill and wastewater treatment. Compared to Fig. 7 the distribution of emissions looks quite different. This is partly because Fig. 7 shows the sphere of influence of the larger sources for multiple campaigns in different wind directions, and this is particularly prevalent for the landfill to the NW. The distribution of gas leaks below the point source level of the compressor stations is by population distribution, but the surveyed fugitive gas emissions are quite localised to offtake stations that are not in urban locations, the smaller gas governors, or to roadside pipeline leaks, which tend

to be located along a small number of roads. The difference between the inventory emissions distribution is particularly clear for the town of Blackpool, (Fig. S1, and toward the left in Figs. 7 and 12), where very few leaks have been seen in the surveys.

Ryedale has a similar distribution of agricultural and fugitive gas emissions, but there are no point sources and the only waste source in the local inventory is the Malton (Figs. S2 and S10) wastewater treatment plant. Based on multiple surveys there are no significant methane emissions downwind of the wastewater treatment plant, but significant emissions from two landfill sites.

Cow breath and their waste products are often found as a mixed source in cow barns during the surveys. The inventory for 2016

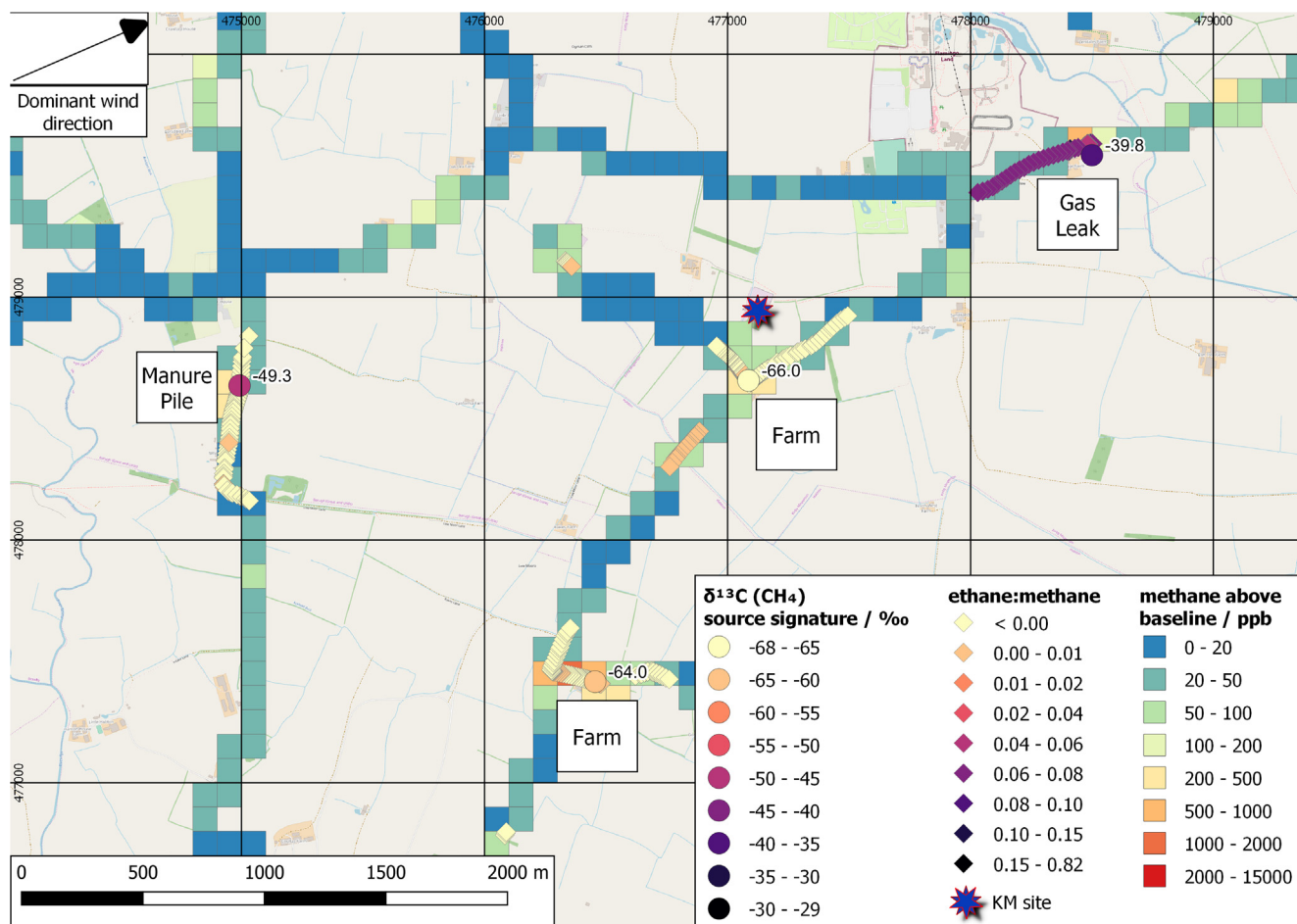


**Fig. 11.** Sources of methane around the KM8 site. The excess methane over background for the 9 survey periods of these roads are binned into 100 × 100 m boxes. Sources sampled are marked as circles with calculated  $\delta^{13}\text{C}$  source signatures adjacent, and the ethane/methane ratios are shown as the narrower trails. Base map provided by © OpenStreetMap contributors.

(from <http://naei.beis.gov.uk/> on 14-Sep-18) indicates that on average only 16.4% of the emission is from the waste product, suggesting that we should be observing an isotopic signature around  $-66.7\text{‰}$  for occupied cow barns given the end member signatures of  $-70\text{‰}$  for breath and  $-50\text{‰}$  for waste. Signatures were close to this for 2017–18 Ryedale surveys but tend to be more enriched during the Fylde surveys, suggesting different farming practice, which could include use of dietary supplements that include C4 plants (enriched in  $^{13}\text{C}$ ) such as maize.

#### 4.6. Potential for identification of fugitive emissions from shale gas extraction

The global database of Sherwood et al., 2017 gives a  $\delta^{13}\text{C}$  range of  $-70$  to  $-24\text{‰}$  with a median  $-41\text{‰}$  for shale gases, compared to  $-42\text{‰}$  for conventional gases ( $-42$  to  $-39\text{‰}$  in the Fylde and Ryedale regions), although most developments are clustered in the thermogenic range, e.g.  $-46$  to  $-35\text{‰}$  for Fayetteville and Barnett shales (Qu et al., 2016). The C2:C1 ratio may provide a clearer separation from the conventional gas network leaks. Globally the range for shale gas is 0 to 0.39, with a median of 0.016 (Sherwood et al., 2017), compared to the range of 0.055 to 0.085 for the Fylde and Ryedale gas supplies. The gases in, and extracted from, the Bowland Shale target formations beneath the Fylde region have been investigated by Clarke et al. (2018). Samples have  $\delta^{13}\text{C}$  of  $-39.8$  to  $-39.7\text{‰}$  and C2:C1 ratios of 0.006 to 0.07, overlapping the ranges for the current gas distribution network. Cuadrilla (2019) report an average composition from their gas analysis tests

that gives a ratio of 0.017, so there is the likelihood that a clear distinction can be made.

## 5. Recommendations and future campaigns

Individual surveys in a region capture just a snapshot of activities. Surveying on the closest driveable route means that emissions may be missed due to wind direction and proximity to source. Fixed daily events such as cow milking in barns may be missed, or encountered by chance at some farms depending on the survey route. Carrying out two-day surveys in each region mostly alleviated this, and allowed more of the sources around each drilling site to be mapped. Given the dominance of westerly airflow in the UK, multiple surveys in each region were needed in order to capture the less prevalent easterly airflow and additional sources. The value of multiply repeated surveys is also clear when analysing the isotopic data. Patterns and trends start to emerge and allow the production of Miller-Tans plots with improved precision, necessary to independently identify any additional fugitive emissions from unconventional gas extraction in these complex source environments.

Detection of small gas leaks can be problematic. The RHUL survey vehicle has the inlet above the roof at approximately 1.8 m above ground and this is good for surveying larger emission plumes, particularly considering that roadside hedgerows in much of the UK are at a similar height. The method often used for gas leak surveys, because many are small point sources from the roads, is to have the inlet on the front bumper of the vehicle at  $<0.5$  m

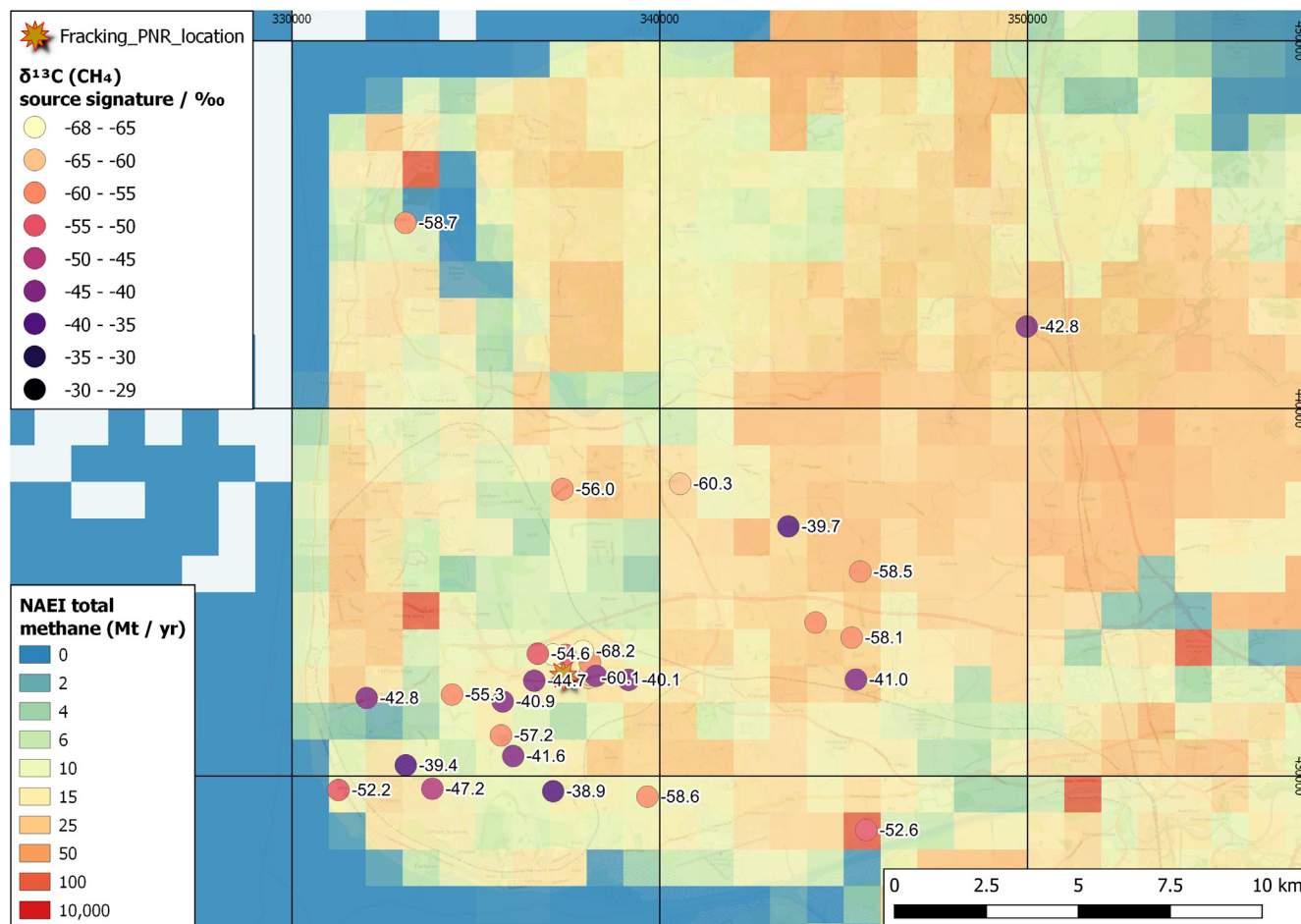


**Fig. 12.** NAEI 2016 inventory for the Fylde region on a 1 × 1 km grid compared to the location of sampled sources. Most sources are found in areas with expected moderate methane emissions, mostly classed as dispersed agricultural sources. There were no sampled sources where emissions were expected to be very low. Base map provided by © OpenStreetMap contributors.

height, and this works well if gas pipes are beneath the roads (eg. Von Fischer et al., 2017). In the UK the pipes are mostly beneath the pavement or roadside verges, with emissions from leaks often through roadside storm drains. These are sometimes seen on one transect, but they are much smaller or not detected on the return transect 5 m away on the other side of the road, even when the wind is carrying the plume across the road. Very close to the source this could be lofted by vehicle turbulence to the 1.8 m inlet height before being carried off in the opposite direction by the prevailing wind. The optimum inlet height for regional multi-source surveys is still under debate and multi-instrument surveys using different heights will be used to test for differences and provide quantifications during some future surveys.

Surveying overnight was considered at the start of the project because the encountered source plumes would have a greater enhancement under inversion conditions. These occurred on cold mornings when associated low wind speeds overnight led to the development of well-defined inversions, which in some instances did not break up until approaching noon. In these instances the regional greenhouse gas emissions mixed together and produced an elevated CH<sub>4</sub> background reaching up to 2.5 ppm after dawn. In such cases the emissions peaks were superimposed on top of an elevated and changing background and often represented merging of plumes from adjacent sources. As a result part of some surveys were not used in the final analysis because there was not a clear separation of source plumes and their chemical signatures.

Further surveys in these regions during 2019 and 2020 will continue to refine the techniques of analysis, with more work to quantify the emission plumes that are observed under optimum conditions. This will be combined with a move toward more in-car data evaluation.

## 6. Conclusions

The main methane sources within a 10 km radius of the PNR and KM drill sites have persisted throughout the baseline study period during 2016 to 2019. These can be grouped as fugitive gas network emissions, waste sources and farm sources. Both the PNR and KM sites have multiple gas and farm sources within 2 km that can influence the measurements at the fixed baseline stations depending on wind direction. Therefore it is key to distinguish these biogenic sources from the thermogenic gas leaks. Using  $\delta^{13}\text{C}$  of methane and ethane:methane (C<sub>2</sub>:C<sub>1</sub>) ratios as proxies clearly separates these source types, with  $\delta^{13}\text{C}$  further subdividing animal waste from animal eructations.

Landfill sites are the largest area source and emissions can be detected many km downwind, sometimes masking plumes from smaller sources. Closure of active landfills during the survey period has been accompanied by a significant reduction in the size of emissions peaks. Cow barns are the focus of farm emissions, often detected up to 500 m downwind, representing a mix of animal

eructations and manure emissions. Spatial distribution varies with season and climate, with more dispersed animal emissions from fields and regular sites populated by manure piles outside of the winter months. The largest gas network emissions are from above ground infrastructure detected more than 1 km downwind, persisting throughout the survey period with small pipeline leaks that are not remediated.

Unconventional gas extraction had not started during the survey period, but the baseline presented here provides a context of existing sources of methane in the local areas of the UK's furthest-developed shale gas wells. In addition, the baseline facilitates the future discrimination of emissions attributable to shale gas extraction from extraneous local sources by analysis of isotopic or ethane:methane (C<sub>2</sub>:C<sub>1</sub>) proxies, although this would not be definitive until production samples are available for comparison.

### CRedit authorship contribution statement

**David Lowry:** Conceptualization, Methodology, Investigation, Formal analysis, Supervision, Validation, Writing - original draft, Writing - review & editing, Project administration. **Rebecca E. Fisher:** Conceptualization, Methodology, Investigation, Formal analysis, Supervision, Validation, Writing - original draft, Writing - review & editing. **James L. France:** Methodology, Investigation, Formal analysis, Supervision, Validation, Writing - original draft, Writing - review & editing, Data curation. **Max Coleman:** Investigation, Formal analysis, Writing - review & editing. **Mathias Lanoisellé:** Investigation. **Giulia Zazzeri:** Investigation, Formal analysis, Writing - review & editing. **Euan G. Nisbet:** Conceptualization, Writing - review & editing. **Jacob T. Shaw:** Investigation, Writing - review & editing. **Grant Allen:** Conceptualization, Investigation, Writing - review & editing. **Joseph Pitt:** Investigation. **Robert S. Ward:** Conceptualization, Funding acquisition, Project administration, Writing - review & editing.

### Declaration of Competing Interest

The authors declare that they have no known competing financial interests or personal relationships that could have appeared to influence the work reported in this paper.

### Acknowledgements

Thanks to Jerry Morris of the RHUL science workshop who set-up and adapted the survey vehicle to accommodate the multiple instruments, power supplies and roof ornaments. This ongoing research is funded by the UK Government Department for Business, Energy and Industrial Strategy (BEIS; Grant code: GA/18F/017/NEE6617R). BGS authors publish with the permission of the Executive Director, BGS NERC-UKRI. The project has close synergies with the NERC-funded Equipt4Risk project. The measurement protocols for this project are closely linked to those that have been developed for the EU Horizon 2020 Marie Skłodowska-Curie Innovative Training Network MEMO<sup>2</sup> (MEthane goes MOBILE: MEasurement and MOdelling). OpenStreetMap<sup>®</sup> is used to create the basemaps for most figures. It is *open data*, licensed under the [Open Data Commons Open Database License](https://www.openstreetmap.org/copyright) (ODbL) by the [OpenStreetMap Foundation](https://www.openstreetmap.org/copyright) (OSMF). Data is available under the Open Database Licence, and map tiles licenced as CC BY-SA. <https://www.openstreetmap.org/copyright>

### Appendix A. Supplementary data

Supplementary data to this article can be found online at <https://doi.org/10.1016/j.scitotenv.2019.134600>.

### References

- Alvarez, R.A., Zavala-Araiza, D., Lyon, D.R., Allen, D.T., Barkley, Z.R., Brandt, A.R., Davis, K.J., Herndon, S.C., Jacob, D.J., Karion, A., Kort, E.A., Lamb, B.K., Lauvaux, T., Maasakkers, J.D., Marchese, A.J., Omara, M., Pacala, S.W., Peischl, J., Robinson, A. L., Shepson, P.B., Sweeney, C., Townsend-Small, A., Wofsy, S.C., Hamburg, S.P., 2018. Assessment of methane emissions from the U.S. oil and gas supply chain. *Science* 361 (6398), 186–188. <https://doi.org/10.1126/science.aar7204>.
- Boothroyd, I.M., Almond, S., Qassim, S.M., Worrall, F., Davies, R.J., 2016. Fugitive emissions of methane from abandoned, decommissioned oil and gas wells. *Sci. Total Environ.* 547, 461–468. <https://doi.org/10.1016/j.scitotenv.2015.12.096>.
- Boothroyd, I.M., Almond, S., Worrall, F., Davies, R.J., 2017. Assessing the fugitive emission of CH<sub>4</sub> via migration along fault zones—Comparing potential shale gas basins to non-shale basins in the UK. *Sci. Total Environ.* 580, 412–424. <https://doi.org/10.1016/j.scitotenv.2016.09.052>.
- Boothroyd, I.M., Almond, S., Worrall, F., Davies, R.K., Davies, R.J., 2018. Assessing fugitive emissions of CH<sub>4</sub> from high-pressure gas pipelines in the UK. *Sci. Total Environ.* 631–632, 1638–1648. <https://doi.org/10.1016/j.scitotenv.2018.02.240>.
- Clarke, H., Turner, P., Bustin, R.M., Riley, N., Besly, B., 2018. Shale gas resources of the Bowland Basin, NW England: a holistic study. *Pet. Geosci.* 24, 287–322. <https://doi.org/10.1144/petgeo2017-066>.
- Cuadrilla, 2019. Preston New Road-1z: LJ/06-09(z) HFP Report, Cuadrilla Bowland Limited, 25pp.
- Dlugokencky, E.J., Nisbet, E.G., Fisher, R.E., Lowry, D., 2011. Global atmospheric methane: budget, changes, and dangers. *Phil. Trans. R. Soc. A* 369, 2058–2072. <https://doi.org/10.1098/rsta.2010.0341>.
- Fisher, R., Lowry, D., Wilkin, O., Srisankarajah, S., Nisbet, E.G., 2006. High-precision, automated stable isotope analysis of atmospheric methane and carbon dioxide using continuous-flow isotope-ratio mass spectrometry. *Rapid Commun. Mass Spectrom.* 20, 200–208. <https://doi.org/10.1002/rcm.2300>.
- France, J.L., Cain, M., Fisher, R.E., Lowry, D., Allen, G., O'Shea, S.J., Illingworth, S., Pyle, J., Warwick, N., Jones, B.T., Gallagher, M.W., Bower, K., Le Breton, M., Percival, C., Muller, J., Welpott, A., Baugitte, S., George, C., Hayman, G.D., Manning, A.J., Lund-Myrhe, C., Lanoisellé, M., Nisbet, E.G., 2016. Measurements of  $\delta^{13}\text{C}$  in CH<sub>4</sub> and using particle dispersion modeling to characterize sources of Arctic methane within an air mass. *J. Geophys. Res.: Atmos.* 121, 4257–4270. <https://doi.org/10.1002/2016JD026006>.
- Hitchman, S.P., Darling, W.G., Williams, G.M., 1989. Stable isotope ratios in methane containing gases in the United Kingdom. *Brit. Geol. Surv. Tech. Rep.*, WE189130.
- Karion, A., Sweeney, C., Pétron, G., Frost, G., Hardesty, R.M., Kofler, J., Miller, B.R., Newberger, T., Wolter, S., Banta, R., Brewer, A., Dlugokencky, E., Lang, P., Montzka, S.A., Schnell, R., Tans, P., Trainer, M., Zamora, R., Conley, S., 2013. Methane emissions estimate from airborne measurements over a western United States natural gas field. *Geophys. Res. Lett.* 40, 4393–4397. <https://doi.org/10.1002/grl.50811>.
- Keeling, C.D., 1961. The concentration and isotopic abundance of carbon dioxide in rural and marine air. *Geochim. et Cosmochim. Acta* 24, 277–298.
- Liptay, K., Chanton, J., Czepl, P., Moher, B., 1998. Use of stable isotopes to determine methane oxidation in landfill cover soils. *J. Geophys. Res.: Atmos.* 103, 8243–8250. <https://doi.org/10.1029/97JD02630>.
- Lopez, M., Sherwood, O.A., Dlugokencky, E.J., Kessler, R., Giroux, L., Worthy, D.E.J., 2017. Isotopic signatures of anthropogenic CH<sub>4</sub> sources in Alberta, Canada. *Atmos. Environ.* 164, 280–288. <https://doi.org/10.1016/j.atmosenv.2017.06.021>.
- Lowry, D., Holmes, C.W., Rata, N.D., O'Brien, P., Nisbet, E.G., 2001. London methane emissions: use of diurnal changes in concentration and  $\delta^{13}\text{C}$  to identify urban sources and verify inventories. *J. Geophys. Res.: Atmos.* 106, 7427–7448. <https://doi.org/10.1029/2000JD900601>.
- Miller, J.B., Tans, P.P., 2003. Calculating isotopic fractionation from atmospheric measurements at various scales. *Tellus B* 55, 2207–2214. <https://doi.org/10.1034/j.1600-0889.2003.00020.x>.
- McKay, D.J.C., Stone, T.J., 2013. Potential Greenhouse Gas Emissions Associated with Shale Gas Extraction and Use. Department of Energy and Climate Change, London, URN 13D/230, 50pp.
- NAEI 2019. © Crown 2019 copyright Defra & BEIS via [naei.beis.gov.uk](http://naei.beis.gov.uk), licenced under the Open Government Licence (OGL).
- O'Shea, S.J., Allen, G., Fleming, Z.L., Bauguitte, S.J.-B., Percival, C.J., Gallagher, M.W., Lee, J., Helfter, C., Nemitz, E., 2014. Area fluxes of carbon dioxide, methane, and carbon monoxide derived from airborne measurements around Greater London: A case study during summer 2012. *J. Geophys. Res.: Atmos.* 119, 4940–4952. <https://doi.org/10.1002/2013JD021269>.
- Pataki, D.E., Bowling, D.R., Ehleringer, J.R., 2003. Seasonal cycle of carbon dioxide and its isotopic composition in an urban atmosphere: anthropogenic and biogenic effects. *J. Geophys. Res.: Atmos.* 108, 4735. <https://doi.org/10.1029/2003JD003865>.
- Peischl, J., Ryerson, T.B., Aikin, K.C., de Gouw, J.A., Gilman, J.B., Holloway, J.S., Lerner, B.M., Nadkarni, R., Neuman, J.A., Nowak, J.B., Trainer, M., Warneke, C., Parrish, D. D., 2015. Quantifying atmospheric methane emissions from the Haynesville, Fayetteville, and northeastern Marcellus shale gas production regions. *J. Geophys. Res.: Atmos.* 120, 2119–2139. <https://doi.org/10.1002/2014JD022697>.
- Phillips, N.G., Ackley, R., Crosson, E.R., Down, A., Hutryra, L.R., Bronfield, M., Karr, J. D., Zhao, K., Jackson, R.B., 2013. Mapping urban pipeline leaks: methane leaks across Boston. *Environ. Pollut.* 173, 1–4. <https://doi.org/10.1016/j.envpol.2012.11.003>.

- Priestley, S., 2018. Shale Gas and Fracking. Briefing Paper CBP 6073, House of Commons. Library, 40.
- Purvis, R.M., Lewis, A.C., Hopkins, J.R., Wilde, S.E., Dunmore, R.E., Allen, G., Pitt, J., Ward, R.S., 2019. Effects of pre-fracking operations on ambient air quality at a shale gas exploration site in rural North Yorkshire, England. *Sci. Total Environ.* 673, 445–454. <https://doi.org/10.1016/j.scitotenv.2019.04.077>.
- Qu, Z., Sun, J., Shi, J., Zhan, Z., Zhou, Y., Peng, P., 2016. Characteristics of stable carbon isotopic composition of shale gas. *J. Nat. Gas Geosci.* 1, 147–155. <https://doi.org/10.1016/j.jnggs.2016.05.008>.
- Rella, C.W., Tsai, T.R., Botkin, C.G., Crosson, E.R., Steele, D., 2015a. Measuring emissions from oil and natural gas well pads using the mobile flux plane technique. *Environ. Sci. Technol.* 49, 4742–4748. <https://doi.org/10.1021/acs.est.5b00099>.
- Rella, C.W., Hoffnagle, J., He, Y., Tajuma, S., 2015b. Local- and regional-scale measurements of CH<sub>4</sub>, δ<sup>13</sup>C, and C<sub>2</sub>H<sub>6</sub> in the Uintah Basin using a mobile stable isotope analyzer. *Atmos. Meas. Tech.* 8, 4539–4559. <https://doi.org/10.5194/amt-8-4539-2015>.
- Röckmann, T., Eyer, S., van der Veen, C., Popa, M.E., Tuzson, B., Monteil, G., Houweling, S., Harris, E., Brunner, D., Fischer, H., Zazzeri, G., Lowry, D., Nisbet, E. G., Brand, W.A., Necki, J.M., Emmenegger, L., Mohn, J., 2016. In situ observations of the isotopic composition of methane at the Cabauw tall tower site. *Atmos. Chem. Phys.* 16, 10469–10487. <https://doi.org/10.5194/acp-16-10469-2016>.
- Rust, F., 1981. Ruminant methane delta (<sup>13</sup>C/<sup>12</sup>C) values: relation to atmospheric methane. *Science* 211 (4486), 1044–1046. <https://doi.org/10.1126/science.7466376>.
- Schweitzke, S., Sherwood, O.A., Bruhwiler, L.M.P., Miller, J.B., Etiope, G., Dligokency, E.J., Englund Michel, S., Arling, V.A., Vaughn, B.H., White, J.W.C., Tans, P.P., 2016. Upward revision of global fossil fuel methane emissions based on isotope database. *Nature* 538, 88–91. <https://doi.org/10.1038/nature19797>.
- Shaw, J.T., Allen, G., Pitt, J., Mead, M.I., Purvis, R.M., Dunmore, R., Wilde, S., Shaf, A., Barker, P., Bateson, P., Bacak, A., Lewis, A.C., Lowry, D., Fisher, R., Lanoisellé, M., Ward, R.S., 2019. A baseline of atmospheric greenhouse gases for prospective UK shale gas sites. *Sci. Total Environ.* 684, 1–13. <https://doi.org/10.1016/j.scitotenv.2019.05.266>.
- Sherwood, O., Schweitzke, S., Arling, V.A., Etiope, G., 2017. Global inventory of gas geochemistry data from fossil fuel, microbial and burning sources, version 2017. *Earth Syst. Sci. Data* 9, 639–656. <https://doi.org/10.5194/essd-9-639-2017>.
- Strapoć, D., Mastalerz, M., Eble, C., Schimmelmann, A., 2007. Characterization of the origin of coalbed gases in southeastern Illinois Basin by compound-specific carbon and hydrogen stable isotope ratios. *Org. Geochem.* 38, 267–287. <https://doi.org/10.1016/j.orggeochem.2006.09.005>.
- Von Fischer, J., Cooley, D., Chamberlain, S., Gaylor, A., Griebenow, C.J., Hamburg, S.P., Salo, J., Schumacher, R., Theobald, D., Ham, J., 2017. Rapid, vehicle-based identification of location and magnitude of urban natural gas pipeline leaks. *Environ. Sci. Technol.* 51, 4091–4099. <https://doi.org/10.1021/acs.est.6b06099>.
- Ward, R.S., Smedley, P.L., Allen, G., Baptie, B.J., Daraktchieva, Z., Horleston, A., Jones, D.G., Jordan, C.J., Lewis, A., Lowry, D., Purvis, R.M., Rivett, M.O., 2017. Environmental Baseline Monitoring Project: Phase II Final Report. British Geological Survey, Nottingham, UK (163 pp. (OR/17/049) (Unpublished)).
- Ward, R.S., Smedley, P.L., Allen, G., Baptie, B.J., Cave, M.R., Daraktchieva, Z., Fisher, R., Hawthorn, D., Jones, D.J.G., Lewis, A., Lowry, D., Luckett, R., Marchant, B.P., Purvis, R.M., Wilde, S., 2018. Environmental Baseline Monitoring: Phase III Final Report (2017–2018). British Geological Survey, Nottingham, UK (143pp. (OR/18/026) (Unpublished)).
- Xiao, Y., Logan, J.A., Jacob, D.J., Hudman, R.C., Yantosca, R., Blake, D.R., 2008. Global budget of ethane and regional constraints on U.S. sources. *J. Geophys. Res.: Atmos.* 113, D21306. <https://doi.org/10.1029/2007JD009415>.
- Zavala-Araiza, D., Lyon, D., Alvarez, R.A., Palacios, V., Harriss, R., Lan, X., Talbot, R., Hamburg, S.P., 2015. Toward a functional definition of methane super-emitters: application to natural gas production sites. *Environ. Sci. Technol.* 49, 8167–8174. <https://doi.org/10.1021/acs.est.5b00133>.
- Zazzeri, G., Lowry, D., Fisher, R.E., France, J.L., Lanoisellé, M., Nisbet, E.G., 2015. Plume mapping and isotopic characterisation of anthropogenic methane sources. *Atmos. Environ.* 110, 151–162. <https://doi.org/10.1016/j.atmosenv.2015.03.029>.
- Zazzeri, G., Lowry, D., Fisher, R.E., France, J.L., Lanoisellé, M., Kelly, B.F.J., Necki, J.M., Iverach, C.P., Ginty, E., Zimnoch, M., Jasek, A., Nisbet, E.G., 2016. Carbon isotopic signature of coal-derived methane emissions to atmosphere: from coalification to alteration. *Atmos. Chem. Phys.* 16, 13669–13680. <https://doi.org/10.5194/acp-16-13669-2016>.
- Zazzeri, G., Lowry, D., Fisher, R.E., France, J.L., Lanoisellé, M., Grimmond, C.S.B., Nisbet, E.G., 2017. Evaluating methane inventories by isotopic analysis in the London region. *Sci. Rep.* 7, 4854. <https://doi.org/10.1038/s41598-017-04802-6>.